

**Strain engineering and bioprocessing strategies for biobased
production of porphobilinogen in *Escherichia coli***

by
Davinder Lall

A thesis
presented to the University of Waterloo
in fulfilment of the
thesis requirement for the degree of
Master of Applied Science
in
Chemical Engineering

Waterloo, Ontario, Canada, 2021

© Davinder Lall 2021

Author's declaration

This thesis consists of material all of which I authored or co-authored: see Statement of Contributions included in the thesis. This is a true copy of the thesis, including any required final revisions, as accepted by my examiners.

I understand that my thesis may be made electronically available to the public.

Statement of Contributions

Davinder Lall was the sole author for the thesis which was written under the supervision of Dr. C Perry Choy and Dr. Murray Moo-Young.

This thesis consists in part of a manuscript written for publication.

Research presented in the thesis:

This research was conducted at the University of Waterloo by Davinder Lall under the supervision of Dr. C Perry Chou and Dr. Murray Moo-Young. As lead author of the chapters, I was responsible for contributing to conceptualizing study design, carrying out data collection and analysis, and drafting and submitting manuscript. My coauthors provided guidance during the research phase and provided feedback on draft manuscripts.

Citations:

Davinder Lall, Dragan Miscevic, Mark Bruder, Adam Westbrook, Marc Aucoin, Murray Moo-Young, C. Perry Chou. 2021. Strain engineering and bioprocessing strategies for biobased production of porphobilinogen in *Escherichia coli*. *Bioresources and Bioprocessing*. DOI - 10.1186/s40643-021-00482-3. (Accepted for publication).

Abstract

Strain engineering and bioprocessing strategies were applied for biobased production of porphobilinogen (PBG) using *Escherichia coli* as the cell factory. The non-native Shemin/C4 pathway was first implemented by heterologous expression of *hemA* from *Rhodopseudomonas spheroids* to supply carbon flux from the natural tricarboxylic acid (TCA) pathways for PBG biosynthesis via succinyl-CoA. Metabolic strategies were then applied for carbon flux direction from the TCA pathways to the C4 pathway. To promote PBG stability and accumulation, Clustered Regularly Interspersed Short Palindromic Repeats interference (CRISPRi) was applied to repress *hemC* expression and, therefore, reduce carbon flowthrough toward porphyrin biosynthesis with minimal impact to cell physiology. To further enhance PBG biosynthesis and accumulation under the *hemC*-repressed genetic background, we further heterologously expressed native *E. coli hemB*. Using these engineered *E. coli* strains for bioreactor cultivation based on $\sim 30 \text{ g L}^{-1}$ glycerol, we achieved high PBG titers up to 209 mg L^{-1} , representing 1.73% of the theoretical PBG yield, with improved PBG stability and accumulation. Potential biochemical, genetic, and metabolic factors limiting PBG production were systematically identified for characterization.

Acknowledgements

I would like to use this opportunity to present my sincere gratitude to my supervisors, Dr. C. Perry Chou and Dr. Murray Moo-Young. Dr. Chou provided me with plethora of opportunities, projects, and great guidance through out my research work. His academic and professional understanding, valuable feedbacks, and amazing mentorship helped me boost my confidence, improve my learning curve, embrace failures, and develop scientific expertise. Dr. Murray Moo-Young has always been an inspiration to keep moving forward and try contributing to science as much as possible. I feel proud to have Dr. Chou and Dr. Young as my supervisors.

I extensively thank Dr. Marc Aucoin and Dr. Valerie Ward for serving in my thesis committee and spending precious time to review my written thesis and providing valuable feedback. I would also like to extend my thanks to all the hard-working staff members of Chemical Engineering department as their important role was crucial for success amid global Covid'19 pandemic.

I vastly appreciate Dragan Miscevic for providing excellent technical training, discussing scientific concepts, and superb mentorship to help me establish as an independent researcher in Dr. Chou's research group. Further, I appreciate all the support I received from amazing lab members – Adam, Tesh, Bahareh, and Mohammad, my office partner – Azin, Mark from Dr. Aucoin's lab and co-op/exchange students. Their marvelous friendship and companionship were pinnacle part of life in lab.

Finally, I am deeply grateful to all my friends (in India, Canada, and abroad) and my family for their persistent support and faith in me which kept me motivated to focus on my academic career and strongly face all the challenges.

Dedication

I dedicate my dissertation work to my parents and lovely sisters.

Table of contents

Author's declaration.....	ii
Statement of contributions.....	iii
Abstract.....	iv
Acknowledgements	v
Dedication.....	vi
List of figures	ix
List of tables	x
List of abbreviations	xi
List of symbols	xii
Chapter 1 – Introduction	1
1.1 - Research objective	4
Chapter 2 – Literature review.....	7
2.1 - Background - Biofuels.....	7
2.2 - Biomass conversion technologies.....	9
2.3 - Engineering of natural TCA cycle for bio-based chemical production.....	10
2.4 - Relevant heterologous pathway - Heme biosynthetic pathway.....	11
2.5 - Glycerol as a carbon feedstock.....	14
Chapter 3 - Materials and methods	15
3.1 - Bacterial strains and plasmids	15
3.2 - Media and bacterial cell cultivation.....	19
3.3 - Analysis.....	20
3.4 - Real-time quantitative reverse transcription PCR (qRT-PCR)	21
3.5 - Statistical analysis	22
Chapter 4 – Results	23
4.1 - Shake-flask cultivation for PBG bioproduction.....	23
4.2 - Carbon flux direction from the TCA pathways to the Shemin/C4 pathway.....	26
4.3 - Repression of <i>hemC</i> expression for PBG biosynthesis and accumulation	30
4.4 - Increasing <i>hemB</i> expression to enhance PBG biosynthesis and accumulation.....	32
4.5 - Strain engineering for PBG biosynthesis under microaerobic conditions.....	39

Chapter 5 – Discussion	43
Chapter 6 – Conclusions	47
References	48
Appendix A: Supplementary Tables.....	56

List of figures

Figure 1. Schematic representation of the natural metabolism and the implemented Shemin pathway for PBG and porphyrin biosynthesis in <i>E. coli</i> from glycerol.....	5
Figure 2. Different generations of biofuels.....	9
Figure 3. The C4 pathway for heme biosynthesis.	13
Figure 4. Molecular strategy for CRISPRi-based <i>hemC</i> repression.....	17
Figure 5. Shake flask cultivation of BW Δ <i>ldhA</i> , DMH, DSL and other derived <i>hemC</i> -repressed strains for PBG extracellular accumulation.....	25
Figure 6. Bioreactor cultivation of DMH, DMH Δ <i>sdhA</i> , and DMH Δ <i>iclR</i> for PBG biosynthesis under aerobic conditions.....	29
Figure 7. Bioreactor cultivation of DMH Δ <i>iclR</i> Δ <i>sdhA</i> and DMH-D9 Δ <i>iclR</i> Δ <i>sdhA</i> for PBG biosynthesis under aerobic conditions.....	31
Figure 8. Bioreactor cultivation of DSL, DSL Δ <i>sdhA</i> , and DSL Δ <i>iclR</i> for PBG biosynthesis under aerobic conditions.....	34
Figure 9. Bioreactor cultivation of DSL Δ <i>iclR</i> Δ <i>sdhA</i> and DSL-D9 Δ <i>iclR</i> Δ <i>sdhA</i> for PBG biosynthesis under aerobic conditions.....	35
Figure 10. Bioreactor cultivation of DSL-D1 Δ <i>iclR</i> Δ <i>sdhA</i> , DSL-D2 Δ <i>iclR</i> Δ <i>sdhA</i> , DSL-D3 Δ <i>iclR</i> Δ <i>sdhA</i> , and DSL-D4 Δ <i>iclR</i> Δ <i>sdhA</i> for PBG biosynthesis under aerobic conditions.....	36
Figure 11. Bioreactor cultivation of DSL-D5 Δ <i>iclR</i> Δ <i>sdhA</i> , DSL-D6 Δ <i>iclR</i> Δ <i>sdhA</i> , DSL-D7 Δ <i>iclR</i> Δ <i>sdhA</i> , and DSL-D8 Δ <i>iclR</i> Δ <i>sdhA</i> for PBG biosynthesis under aerobic conditions.....	37
Figure 12. Quantification of the relative <i>hemC</i> expression for select gRNAs using qRT-PCR....	38
Figure 13. Bioreactor cultivation of DMH, DMH Δ <i>sdhA</i> , and DMH-D9 Δ <i>sdhA</i> for PBG biosynthesis under microaerobic conditions.....	41
Figure 14. Bioreactor cultivation of DSL, DSL Δ <i>sdhA</i> , and DSL-D9 Δ <i>sdhA</i> for PBG biosynthesis under microaerobic conditions.....	42

List of tables

Table 1. <i>E. coli</i> strains and plasmids used in this study.....	18
Table S1: DNA oligonucleotide sequences used in this study.....	56
Table S2: gRNA sequences targeting hemC for CRISPRi in this study.....	57
Table S3: Tabulated images of bioreactor cultivation samples under aerobic and microaerobic conditions.....	58
Table S4: Statistical analysis for comparing experimental data of PBG titers.....	59

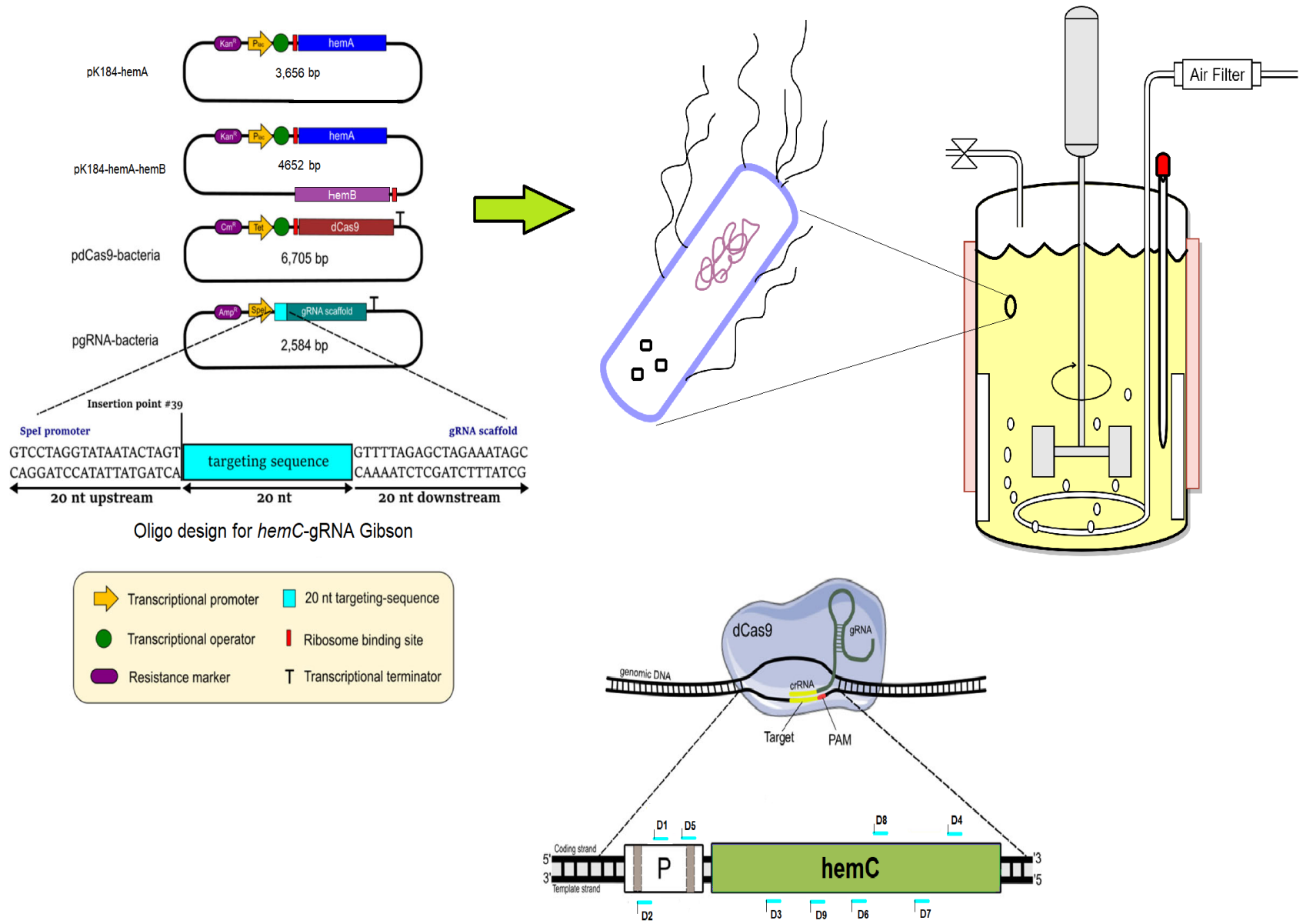
List of abbreviations

5-ALA/ALA	5-Aminolevulinic acid
CoA	Coenzyme A
Cm	Chloramphenicol
CRISPRi	Clustered Regularly Interspersed Short Palindromic Repeats interference
DCW	Dry cell weight
<i>E. coli</i>	<i>Escherichia coli</i>
HemA	ALA synthase from <i>Rhodopseudomonas spheroids</i> (encoded by <i>hemA</i>)
HemB	ALA dehydratase (encoded by <i>hemB</i>)
HemC	porphobilinogen deaminase (PBGD) (encoded by <i>hemC</i>)
HMB	Hydroxymethylbilane
IcIR	transcriptional AceBAK operon repressor (encoded by <i>icIR</i>)
IPTG	Isopropyl β -D-thiogalactopyranoside
Km	Kanamycin
LB	Lysogeny broth
PBG	Porphobilinogen
PWh	petawatt-hour
rpm	revolutions per minute
SdhA	succinate dehydrogenase (SDH) complex flavoprotein subunit A (encoded by <i>sdhA</i>)
TCA	Tricarboxylic acid
vvm	air volume/culture volume/min

List of symbols

Δ	Gene deletion
$^{\circ}$	Degrees of temperature
\pm	Plus-minus (precision of approximation)
α	Alpha subunit
β	Beta subunit
λ	Lambda (indicating wavelength)
μ	Mu (indicating “micro”)
R	Resistance marker

Graphic



Chapter 1

Introduction

Porphobilinogen (PBG) is a pyrrole-containing intermediate in the metabolic pathways for biosynthesis of essential porphyrin/tetrapyrrole compounds known as “pigments of life”, including heme, cobalamin, chlorophyll, siroheme, and heme d₁, etc., in almost all types of biological cells (Frankenberg et al., 2003). For application purposes, PBG can act as a marker for diagnosis of diseases, such as acute intermittent porphyria (Anderson, 2019) and lead (Pb) poisoning (Gibson et al., 1968). Naturally in biological systems, the precursor of PBG, i.e., 5-aminolevulinic acid (5-ALA), is synthesized via either of the two unrelated metabolic routes, i.e., the Beale/C5 pathway and the Shemin/C4 pathway (Zhang et al., 2015). Found in most bacteria (including *Escherichia coli*) and all archaea and plants, the C5 pathway starts with the C5-skeleton of glutamate for conducting two enzymic reactions, i.e., initial reduction of glutamyl-tRNA to glutamate-1-semialdehyde (GSA) via NADPH-dependent glutamyl-tRNA reductase (GluTR) and subsequent transamination of GSA via glutamate-1-semialdehyde-2,1-aminomutase (GSAM), to form 5-ALA (Jahn et al., 1992). On other hand, the C4 pathway, present in humans, animals, fungi and the α -group of proteobacteria, involves ALA synthase (ALAS or HemA, encoded by *hemA*) for molecular condensation of succinyl-CoA and glycine to form 5-ALA with the release of carbon dioxide and coenzyme A (CoA) (Nandi, 1978). Subsequently, PBG is synthesized via a common reaction for molecular condensation of two 5-ALA molecules catalyzed by ALA dehydratase (ALAD or HemB, encoded by *hemB*) (Layer et al., 2010).

Even with relatively limited applicability up to date, technologies for PBG production have been explored. Chemical synthesis of PBG has been carried out using a variety of precursor

molecules, such as diethyl 4-oxopimelate (Jones et al., 1976), 2-methoxy-4-methyl-5-nitropyridine (Frydman et al., 1965), and 2-Hydroxy-4-methyl-5-nitropyridine (Frydman et al., 1969), as well as reaction processes, such as modified synthesis via a porphobilinogen lactam (Kenner et al., 1977), MacDonald's method (Jackson & MacDonald, 1957), and ozonide cleavage reaction (Jacobi & Li, 2001). However, these chemical approaches are expensive, time-consuming, complex, and requiring harsh reaction conditions with typically low yields (Neier, 2000). While purification of PBG from the urine of patients with acute porphyria is feasible, the producing capacity is knowingly limited (Westall, 1952). While biosynthesis of PBG has been alternatively explored in different microbial cell factories, such as *Rhodospseudomonas spheroides* (Hatch & Lascelles, 1972), *E. coli* (Lee et al., 2013), *Chromatium vinosum* (Vogelmann et al., 1975), and *Propionibacterium freudenreichii* etc (Y. Piao et al., 2004), enhancing such biobased production is considered technically challenging since PBG, as a metabolic intermediate, hardly accumulates.

While various cell factories have been developed for biobased production (Chen et al., 2013), bacterium *E. coli* remains the most common one. In native *E. coli*, PBG is synthesized via the C5 pathway and barely accumulates extracellularly since the produced PBG will be readily tetramerized into hydroxymethylbilane (HMB) via porphobilinogen deaminase (PBGD or HemC, encoded by *hemC*) for subsequent biosynthesis of essential porphyrins, such as heme. In this study, we chose to first implement the non-native C4 pathway into *E. coli* for PBG biosynthesis and promote PBG extracellular accumulation, from the structurally unrelated carbon of glycerol by heterologous expression of *hemA* from *R. spheroids* (Figure 1). Recently, glycerol has been recognized as a promising carbon source for biobased production due to its low cost (Ciriminna et al., 2014), abundancy, and high degree of reduction (Westbrook et al., 2019), resulting in high product yield compared to traditional sugars (Dharmadi et al., 2006). We also developed effective

metabolic strategies for carbon flux direction via succinyl-CoA, a key precursor of the C4 pathway. The direction of dissimilated carbon toward succinyl-CoA is dependent on three oxygen-sensitive metabolic routes associated with the central metabolism, i.e., oxidative tricarboxylic acid (TCA) cycle, reductive TCA branch, and glyoxylate shunt (Figure 1) (Cheng et al., 2013). Under oxygen-deprived (i.e., anaerobic) conditions, succinate (the precursor of succinyl-CoA) acts as an electron acceptor in place of oxygen and accumulates as a final product of mixed acid fermentation via the reductive TCA branch (Thakker et al., 2012). Under oxygen-rich (i.e., aerobic) conditions, succinate acts as a metabolic intermediate of the oxidative TCA cycle without accumulation, but it can also be alternatively derived via the glyoxylate shunt (Thakker et al., 2012). Here, we explored the manipulation of select genes involved in the TCA pathways and cultivation conditions to enhance carbon flux direction into the C4 pathway via succinyl-CoA.

To promote PBG accumulation, we had to limit the activity of subsequent PBG-consuming reactions toward porphyrins. Since porphyrin biosynthesis is essential for cell survival, knocking out any of these PBG-consuming reactions would be lethal. Hence, we applied Clustered Regularly Interspersed Short Palindromic Repeats interference (CRISPRi) (Qi et al., 2013) to repress the expression of *hemC*, whose encoding gene product of HemC mediates the conversion of PBG to HMB, with minimal impact to cell physiology. To further enhance PBG biosynthesis and accumulation under the *hemC*-repressed genetic background, we also conducted heterologous coexpression of *hemA* from *R. spheroides* and the native *hemB*. In summary, we demonstrated the application of integrated strain engineering and bioprocessing strategies to enhance biosynthesis and ultimate extracellular accumulation of PBG, with systematic identification of potential biochemical, genetic, and metabolic factors limiting PBG production for characterization.

1.1 Research objectives

The main objectives of this research are outlined as follows:

1. Implement non-native Shemin pathway in *E. coli* for PBG biosynthesis with glycerol as a sole carbon source.
2. Establish metabolic strategies for carbon flux direction from TCA cycle and CRISPRi based *hemC* gene repression for enhanced PBG biosynthesis in *E. coli* under different oxygenic conditions.
3. Introduce heterologous expression of native *E. coli hemB* for further improvement in PBG extracellular accumulation.

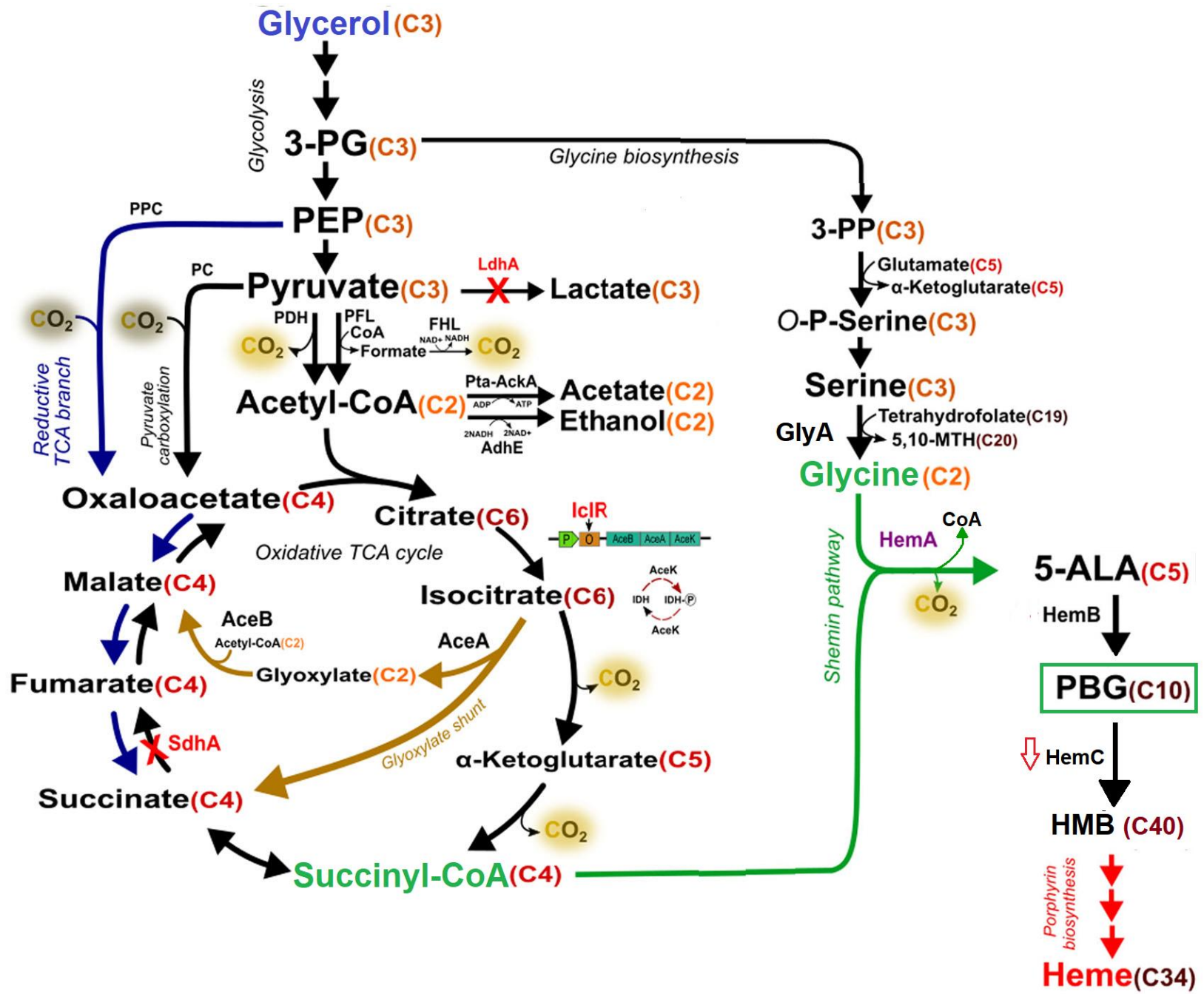


Figure 1. Schematic representation of the natural metabolism and the implemented Shemin pathway for PBG and porphyrin biosynthesis in *E. coli* from glycerol. Metabolic pathways outlined: glycolysis, glycine biosynthesis, pyruvate carboxylation, and oxidative TCA cycle (in black); glyoxylate shunt in the TCA cycle (in light brown); reductive branch of TCA cycle (in blue); Shemin/C4 pathway (in green); porphyrin formation (in red). Colored proteins: mutations (in red); heterologous expression (in purple); carbon source: glycerol (in blue). Metabolite abbreviations: 5,10-MTH, 5,10-methenyltetrahydrofolic acid; 5-ALA, 5-aminolevulinic acid; 3-PG, 3-phosphoglycerate; 3-PP, 3-phosphooxypyruvate; O-P-Serine, O-phospho-L-serine; PBG, porphobilinogen; HMB, hydroxymethylbilane; PEP, phosphoenolpyruvate; CoA, coenzyme A. The number of carbon atoms for each metabolite is specified in orange/red. Protein abbreviations: AceA, isocitrate lyase; AceB, malate synthase A; AceK, isocitrate dehydrogenase kinase/phosphatase; AckA, acetate kinase; AdhE, aldehyde-alcohol dehydrogenase; FHL, formate hydrogenlyase; HemA, 5-aminolevulinate synthase; HemB, 5-aminolevulinate dehydratase; HemC, porphobilinogen deaminase; IclR, AceBAK operon repressor; IDH, isocitrate dehydrogenase; IDH-P, isocitrate dehydrogenase-phosphate; LdhA, lactate dehydrogenase A; PC, pyruvate carboxylase; PckA, phosphoenolpyruvate carboxykinase; PDH, pyruvate dehydrogenase; PFL, pyruvate formate-lyase; PK, pyruvate kinase; PPC, phosphoenolpyruvate carboxylase; Pta, phosphotransacetylase; SdhA, succinate dehydrogenase complex (subunit A).

Chapter 2

Literature Review

2.1 Background- Biofuels

Roughly, 1-2 million years ago humans learned to control fire and with that begin series of changes in their living style and set in motion an early stage for energy demand, which is ever-increasing to this day. Dry leaves, grass, tree bark, branches, dead wood etc. comprised the simple and readily available fuel source for early human civilizations to carry out certain activities like keeping them warm in cold nights, cooking, making tools and weapons for hunting, protection, and agriculture. Then, fast forwarding to industrial age in 18th century, vast quantities of non-renewable resources like natural gas, petroleum, and coal consumption begin to drive industries and shape economies, which still stands true today, as it constitutes a major portion of fuel for meeting energy demands (104.67 PWh on primary energy basis) of around 7.18 billion people around world in 2013 and this energy utilization is expected to rise to 262.8 PWh in near future (2050) [1]. In 2011, around 85% of the energy needs were fulfilled just with fossil fuels [2]. The depleting nature of non-replenishable resources, increasing threat of Green House Gases (GHGs) emissions and other pollutants deteriorating the ecosystem, increasing demand of energy due to population rise and technology-driven lifestyle (Osman et al., 2021) calls for researchers worldwide to search for green and sustainable alternatives. Unlike other renewable energy sources such as wind, solar, geothermal, hydropower, etc., biomass can directly produce fuel and chemicals (Farrell et al., 2020). Moreover, biomass feedstock has other advantages like low dependence on location and climate as they can grow in varied conditions as presence of diversity of vegetation is everywhere, easy storage, and transportation, and low cost associated with waste biomass, etc., thus, biomass

feedstock is a lucrative choice not only for developed nations, but for developing countries in world to counter emerging energy and climatic crisis.

The development of clean and sustainable technologies to convert biomass feedstocks into biofuels is an extensively explored research field. Biofuels are liquid /gaseous fuels manufactured by utilizing biomass feedstocks. They are employed in the transportation sector, generate heat and electricity as well as can be used as the feedstock to synthesise value-added chemicals (Kargbo et al., 2021). Different biomass-based fuels and chemicals like dimethyl ether, ammonia, methane, ethane, propane, butane, ethylene, methanol, ethanol, butanol, acetic acid, gasoline, diesel, paraffin, bio-jet fuels, and many more are produced through various biomass to liquid routes and are sold in the markets throughout the world (Reid et al., 2020). Biofuels are classified as first generation, second generation, third generation and fourth generation biofuels (Demirbas, 2011) (figure 2). The type of biomass used, and process employed determine their composition and calorific content. First generation biofuels like bio-methanol, bioethanol, bio-propanol, bio-butanol, fatty acid esters, etc., are produced from simple sugars, starch, fats and vegetable oils (Naik et al., 2010), but they have disadvantage of causing conflict with global food security (Singh et al., 2011). The second-generation biofuels, such as ethanol are produced by the ‘biomass-to-liquid’ route by using inedible lignocellulosic biomass, i.e., switchgrass and agricultural/forest residues. The third and fourth generation biofuels are part of ‘algae-to-biofuel’ route. In third gen, algal biomass is cultivated for biofuel production whereas metabolic engineering of algae is used for generating biofuels from oxygenic photosynthetic microbes and creating artificial carbon sinks, in fourth generation approach (Lu et al., 2011).

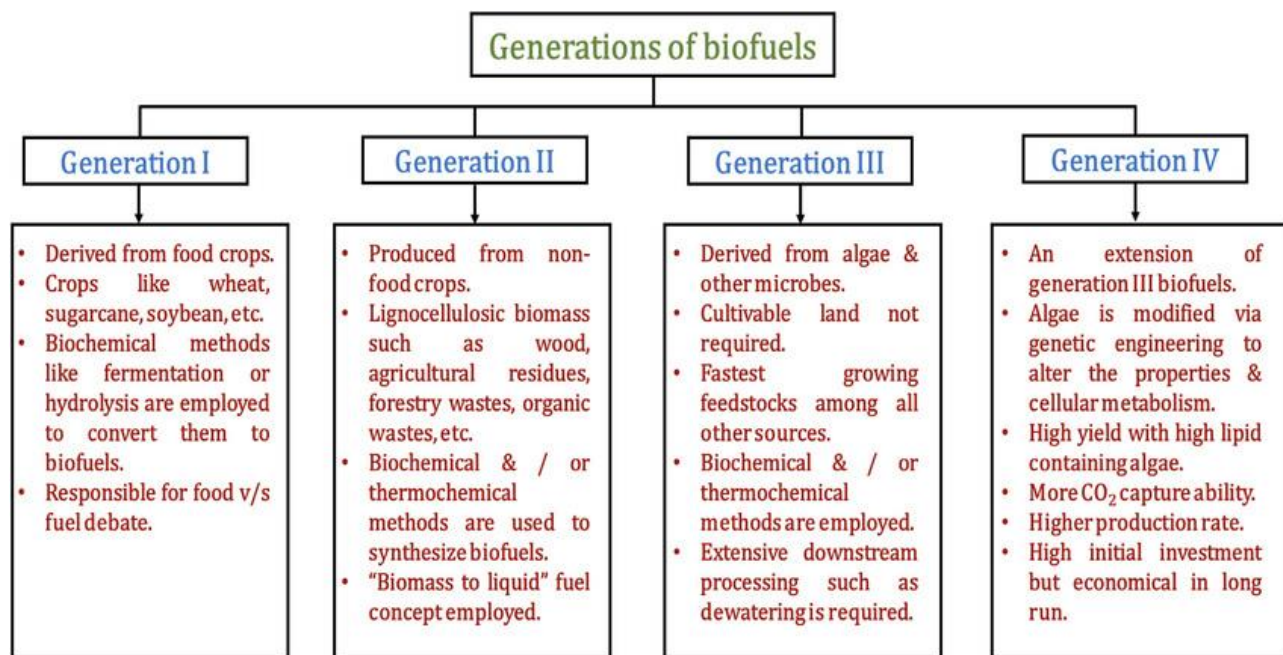


Figure 2. Different generations of biofuels. Image adopted from (Sikarwar et al., 2017).

2.2 Biomass conversion technologies

Due to abundance of biomasses, such as agriculture and domestic wastes, forest residues, industrial wastes, etc., harnessing them is realistically sustainable, reliable, affordable, and full of potential (Ullah et al., 2015). Primordial ways of biomass combustion are not a good method of harnessing energy due environmental and energy output efficiency concerns, but there are other routes namely thermochemical and biochemical, currently in use. Thermochemical methods use heat source and controllable oxygen atmosphere to transform biomass into different energy forms. It is further categorized into (i). combustion, (ii) gasification (where biomass is converted into fuel gas or syngas, which can be cleaned prior to combustion), and (iii) pyrolysis (in absence of oxygen, converts biomass at temperatures around 500 °C to liquid (bio-oil), gaseous and solid (char) fractions. The biochemical methods use biological enzymes, bacteria, or other engineered

microbial systems to transform biomass into liquid fuels like drop-in-biofuels. They majorly comprise processes of digestion, fermentation, and extraction. (Guo et al., 2020).

2.3 Engineering of natural TCA cycle for bio-based chemical production

The TCA cycle is an important biochemical hub of the cell. It has two main functions: generation of energy and synthesis of precursors. The intrinsic problem of lower maximum pathway yields respective to theoretical maximum yields, for instance - for succinate, can be solved metabolically, by creating two pathways to the product by using both branches of the TCA cycle and joining them with the glyoxylate shunt (GS) (Vuoristo et al., 2016). In, fermentation industry, chemicals such as citric acid (Papagianni, 2007), L-glutamic acid (Hermann, 2003), and recently, the production of new chemicals, such as succinic acid (Cao et al., 2013), itaconic acid (Hevekerl et al., 2014), propionic acid (Miscovic et al., 2020), and 1,4-butanediol (Yim et al., 2011) are benefitted by this new metabolic strategy.

Most anaerobic microorganisms producing succinate via the reductive branch of the TCA cycle require two NADH units. But via the glyoxylate shunt, it does not require input of NADH. Product biosynthesis from the oxidative branch of the TCA cycle, such as citric acid and L-glutamic acid, causes reduction in cofactors, and oxygen is needed for NAD⁺ regeneration. Therefore, a combination of both the reductive and oxidative branches of the TCA cycle with glyoxylate shunt proves to be effective as it allows regeneration of cofactors and improve product yield. Thermodynamically, also easy to channel intermediates from the oxidative branch to the reductive branch, as valid for succinate and other product yielding pathways connected at succinyl-CoA node (Vuoristo et al., 2016).

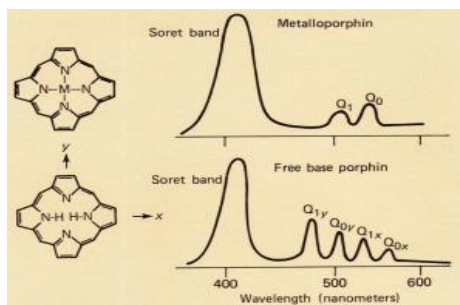
2.4 Relevant heterologous pathway - Heme biosynthetic pathway

Heme biosynthesis is one of highly conserved biochemical pathways existing in all living entities and is thoroughly researched and documented (Layer et al., 2010) (Dailey et al., 2017) (Kwon et al., 2003). The common precursor for biosynthesis porphyrins/tetrapyrroles is 5-aminolevulinic acid (5-ALA), which is preceded by either of the two unrelated metabolic routes - C4 (Shemin) and C5 (or Beale) pathway. Note that all subsequent reactions after 5-ALA formation toward heme are identical. The C5 pathway, found in most bacteria and all archaea and plants, is initiated with ligation step of glutamate and tRNA^{Glu} via glutamyl-tRNA synthase (GluTS). Further, the reduction via glutamyl-tRNA reductase (GluTR) to form glutamate-1-semialdehyde (GSA) occurs. Then, GSA is transaminated by glutamate-1-semialdehyde-2,1-aminomutase (GSAM) to synthesise 5-ALA. Whereas, in the C4 pathway, found in humans, animals, fungi, and some proteobacteria, 5-ALA is produced in a single step reaction catalyzed by 5-ALA synthase (ALAS or HemA) resulting from molecular fusion of succinyl-CoA and glycine (Figure 1 & 3).

The further steps for biosynthesis of various tetrapyrroles/heme (Figure 3) need fusion of two 5-ALA molecules to form the monopyrrole - porphobilinogen (PBG) catalyzed by porphobilinogen synthase (PBGS or HemB). Next, enzyme porphobilinogen deaminase (PBGD or HemC) polymerizes four molecules of PBG to form an unstable intermediate of the linear tetrapyrrole class known as hydroxymethylbilane (HMB). The action of small enzyme called uroporphyrinogen-III synthase (Cosynthase or HemD) perform cyclization of HMB with the inversion of ring D to produce first cyclic tetrapyrrole (porphyrin) intermediate in the heme pathway, i.e., uroporphyrinogen-III (URO-III). The intermediate URO-III forms a major branch/node for various sub-pathways leading to a wide range of porphyrins (Mathews et al., 2001). The decarboxylation step catalyzed by uroporphyrinogen decarboxylase (URO-D or

HemE), yield four methyl groups in a newly formed coproporphyrinogen-III (CPP-III). Here, HemE is the first known decarboxylating enzyme which does not require a cofactor (de Verneuil et al., 1983). The propionate sidechains of CPP-III are converted to vinyl groups by different types of coproporphyrinogen-III oxidases (CPOs), resulting in formation of protoporphyrinogen-IX (PPG-IX). The two different types of CPOs exist - oxygen-dependent HemF and oxygen-independent HemN. Next, a protoporphyrinogen-IX oxidase (PPO or HemG) catalyzes the oxidation of PPG-IX to produce a conjugated double-system tetrapyrrole called protoporphyrin-IX (PP-IX), which is red-pigmented. Lastly, an iron forms a coordination bond with PP-IX catalyzed by ferrochelatase (HemH) to produce heme.

These porphyrins/metalloporphyrins can be analysed with UV-Visible spectrophotometer. At around 405 nm, strong band, called the Soret band, is observed for all porphyrins due to an electron dipole movement that allows $\pi-\pi^*$ transitions. The weaker bands in the region of 500 to 600 nm are called "Q bands. The free base porphyrins show four bands, while metalloporphyrins have only two. The optical absorption spectra can characterize these compounds in solution. Q_0 in metalloporphin is caused by pure electronic transition (with no molecular vibrations) between the electronic ground state and the first electronic excited state whereas Q_1 due to the same electronic transition but with molecular vibrations (called a vibronic band). The subscripts 0 and 1 for free base porphin have a similar interpretation. The x and y subscripts refer to the orientation (polarization) of the electric vector of the absorbed light with respect to the axes shown in diagram.



Spectroscopy of porphyrins (by Kim and Bohandy)

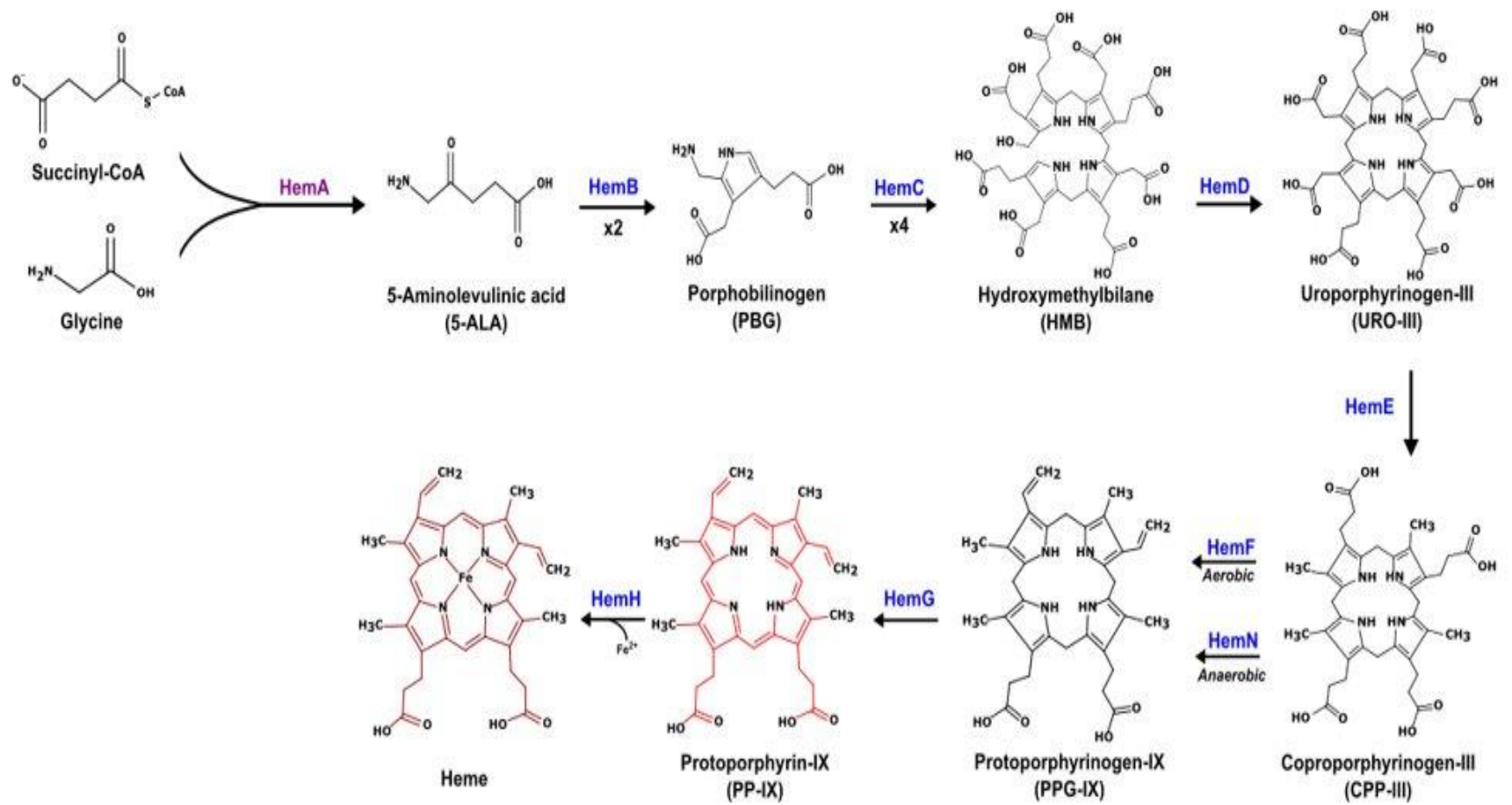


Figure 3. The C4 pathway for heme biosynthesis

2.5 Glycerol as a carbon feedstock

The glycerol feedstock have several advantages over traditional sugars, with high degree of reduction (reductance $\kappa = 4.67$), glycolytic degradation of glycerol can produce nearly twice the number of reducing equivalents (i.e., NADH) in comparison to xylose and glucose ($\kappa = 4$) ((Dharmadi et al., 2006). The glycerol metabolism leads to higher yields, along with wider range of chemicals and fuels that can be produced from microbial systems. Under anaerobic conditions, the metabolic dissimilation of glycerol is negatively affected as the cellular redox balance (the NAD⁺/NADH ratio) must be maintained through terminal transfer of electrons to other metabolic compounds as opposed to molecular oxygen (Gonzalez et al., 2008). Thus, only few organisms (e.g., *Clostridium pasteurianum* and *Klebsiella pneumoniae*) can consume glycerol in anaerobic conditions.

Intracellular glycerol is metabolized either in the presence of electron acceptors (i.e., respiratory branch) or in the absence of electrons acceptors (i.e., fermentative branch) (Gonzalez et al., 2008). Under respiratory conditions, glycerol dissimilation to DHAP (dihydroxyacetone phosphate) follow two different two-step routes, (i) the aerobic GlpK-GlpD pathway, or (ii) the anaerobic GlpK-GlpABC pathway (Blankschien et al., 2010).

Chapter 3

Materials and Methods

3.1 Bacterial strains and plasmids

All bacterial strains and plasmids used in this study are listed in Table 1. Isolation of Genomic DNA from bacterial cells was performed using the Blood & Tissue DNA Isolation Kit (Qiagen, Hilden, Germany). Standard recombinant DNA technologies were applied for molecular cloning (Miller, 1992). Phusion and *Taq* DNA polymerase were obtained from New England Biolabs (Ipswich, MA, USA). All synthesized oligonucleotides were ordered from Integrated DNA Technologies (Coralville, IA, USA). DNA sequencing was performed by the Centre for Applied Genomics at the Hospital for Sick Children (Toronto, Canada). *E. coli* BW25113 was the parental strain for derivation of all engineered strains in this study and DH5 α was used as a *E. coli* host for molecular cloning. The *ldhA* gene encoding lactate dehydrogenase (LDH) was previously inactivated in BW25113, generating BW Δ *ldhA* (K. Srirangan et al., 2014), a strain with much lower byproduct metabolite production.

Genetic implementation of the Shemin/C4 pathway in BW Δ *ldhA* was previously described (Miscovic et al., 2021). Heterologous expression of the *hemA* gene cloned in the pK184 vector was under the control of the P_{lac} promoter. For heterologous coexpression of *hemA* and *hemB* in BW Δ *ldhA*, the native *E. coli* *hemB* gene was first amplified by polymerase chain reaction (PCR) using the primer set g-hemA-hemB and the genomic DNA of BW Δ *ldhA* as the template. The amplified *hemB* gene was Gibson-assembled with PCR-linearized pK184-hemA using the primer set g-pK-hemA-hemB to generate the plasmid pK184-hemA-hemB. Heterologous co-expression of the *hemA* and *hemB* genes cloned in the pK184 vector was also under the control of the P_{lac}

promoter.

Gene knockouts, including *sdhA* (encoding succinate dehydrogenase (SDH) complex flavoprotein subunit A, SdhA) and *iclR* (encoding transcriptional AceBAK operon repressor, IclR), were introduced into BW Δ *ldhA* by P1 phage transduction (Miller, 1992) using the appropriate Keio Collection strains (The Coli Genetic Stock Center, Yale University, New Haven, CT, USA) as donors (Baba et al., 2006). For eliminating the co-transduced FRT-Kn^R-FRT cassette, the transductants were transformed with pCP20 (Cherepanov & Wackernagel, 1995), a temperature sensitive plasmid expressing a flippase (Flp) recombinase. After Flp-mediated excision of the Kn^R cassette, a single Flp recognition site (FRT “scar site”) was generated. The pCP20-containing cells were cured by incubation at 42°C. The genotypes of derived knockout strains were confirmed by colony PCR using the appropriate verification primer sets (Table S1).

Expression of the *hemC* expression was repressed by CRISPRi using various derived plasmids from *pdCas9*-bacteria (Addgene plasmid # 44249) and *pgRNA*-bacteria (Addgene plasmid # 44251). The web tool ChopChop (Labun et al., 2016) was used to design sgRNAs with *hemC*-targeting sequences based on predicted expression efficiencies ranging from approximately 20 to 70% (Table S2). All synthesized oligonucleotide pairs have 60 nucleotides (nt), which include 20 nt *hemC*-targeting sequence, 20 nt upstream and 20 nt downstream sequences of *pgRNA*-bacteria vector (Figure 4). They were annealed as described previously (Pengpumpkiat et al., 2016), generating double-stranded DNA fragments. These DNA fragments were then individually Gibson-assembled with the PCR-linearized *pgRNA*-bacteria using the primer set *gpgRNA* to generate plasmids, such as *pgRNA*-D9 (Table 1). The *hemC*-repressed strains can be developed based on a triple-plasmid system (Figure 4) containing pK184-*hemA* (or pK184-*hemA*-*hemB*), *pdCas9*-bacteria, and the *gRNA*-containing plasmid (such as *pgRNA*-D9).

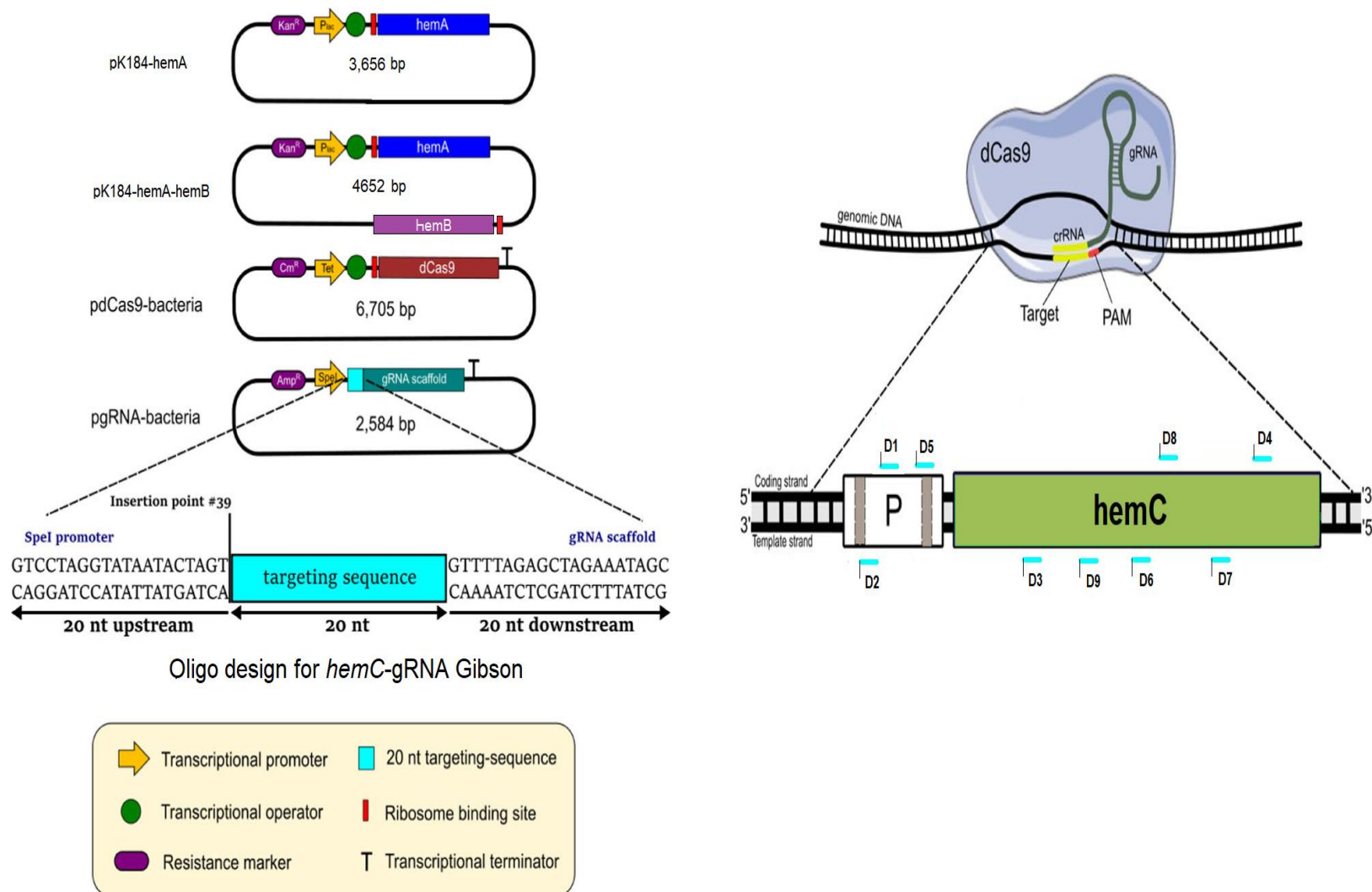


Figure 4. Molecular strategy for CRISPRi-based *hemC* repression. The four plasmids with their major genetic features, such as promoters, antibiotic resistance markers, key genes, for CRISPRi are shown. Select *hemC*-targeting sequences and their associated positions in the *hemC* gene (i.e., D1, D2, D3, D4, D5, D6, D7, D8, and D9) are shown as well. Note that the sequence location, GC content, and predicted *hemC* expression efficiency for various *hemC*-targeting sequences are shown in Table S2, in which select *hemC*-repressed strains derived from *DSLΔiclRΔsdhA* were characterized for quantification of the relative *hemC* mRNA level using qRT-PCR compared to the control *DSLΔiclRΔsdhA* (Figure12). All qRT-PCR experiments were conducted in duplicate.

Table 1. *E. coli* strains and plasmids used in this study

Name	Description or relevant genotype	Source
<i>E. coli</i> host strains		
DH5 α	F ⁻ , <i>endA1</i> , <i>glnV44</i> , <i>thi-1</i> , <i>recA1</i> , <i>relA1</i> , <i>gyrA96</i> , <i>deoR</i> , <i>nupG</i> ϕ 80d <i>lacZ</i> Δ <i>acZd</i> <i>ladlacZYA</i> – <i>argF</i>) <i>U169</i> , <i>hsdR17</i> (rK-mK +), λ -	Lab stock
BW25113	F ⁻ , Δ (<i>araD-araB</i>)567, Δ <i>lacZ</i> 4787(: <i>rrnB-3</i>), λ -, <i>rph-1</i> , Δ (<i>rhaD-rhaB</i>)568, <i>hsdR514</i>	(Datsenko & Wanner, 2000)
BW Δ <i>ldhA</i>	BW25113 <i>ldhA</i> null mutant	(K. Srirangan et al., 2014)
DMH	BW Δ <i>ldhA</i> /pK-hemA	(Miscevic et al., 2021)
DMH Δ <i>sdhA</i>	<i>sdhA</i> null mutant of DMH	(Miscevic et al., 2021)
DMH Δ <i>iclR</i>	<i>iclR</i> null mutant of DMH	This study
DMH Δ <i>iclR</i> Δ <i>sdhA</i>	<i>iclR</i> and <i>sdhA</i> mutants of DMH	(Miscevic et al., 2021)
DMH-D9 Δ <i>sdhA</i>	DMH Δ <i>sdhA</i> /pK-hemA/pgRNA-D9/pdcas9-bacteria	This study
DMH-D9 Δ <i>iclR</i> Δ <i>sdhA</i>	DMH Δ <i>iclR</i> Δ <i>sdhA</i> /pK-hemA/pgRNA-D9/pdcas9-bacteria	This study
DSL	BW Δ <i>ldhA</i> /pK-hemA-hemB	This study
DSL Δ <i>sdhA</i>	<i>sdhA</i> null mutant of DSL	This study
DSL Δ <i>iclR</i>	<i>iclR</i> null mutant of DSL	This study
DSL Δ <i>iclR</i> Δ <i>sdhA</i>	<i>iclR</i> and <i>sdhA</i> mutants of DSL	This study
DSL-D9 Δ <i>sdhA</i>	DSL Δ <i>sdhA</i> /pK-hemA-hemB/pgRNA-D9/pdcas9-bacteria	This study
DMH-CT	DMH /pK-hemA/pgRNA-bacteria/pdcas9-bacteria	This study
DMH-D1	DMH /pK-hemA/pgRNA-D1/pdcas9-bacteria	This study
DMH-D2	DMH /pK-hemA/pgRNA-D2/pdcas9-bacteria	This study
DMH-D3	DMH /pK-hemA/pgRNA-D3/pdcas9-bacteria	This study
DMH-D4	DMH /pK-hemA/pgRNA-D4/pdcas9-bacteria	This study
DSL-CT	DSL /pK-hemA-hemB/pgRNA-bacteria/pdcas9-bacteria	This study
DSL-D1	DSL /pK-hemA-hemB/pgRNA-D1/pdcas9-bacteria	This study
DSL-D2	DSL /pK-hemA-hemB/pgRNA-D2/pdcas9-bacteria	This study
DSL-D3	DSL /pK-hemA-hemB/pgRNA-D3/pdcas9-bacteria	This study
DSL-D4	DSL /pK-hemA-hemB/pgRNA-D4/pdcas9-bacteria	This study
DSL-D1 Δ <i>iclR</i> Δ <i>sdhA</i>	DSL Δ <i>iclR</i> Δ <i>sdhA</i> /pK-hemA-hemB/pgRNA-D1/pdcas9-bacteria	This study
DSL-D2 Δ <i>iclR</i> Δ <i>sdhA</i>	DSL Δ <i>iclR</i> Δ <i>sdhA</i> /pK-hemA-hemB/pgRNA-D2/pdcas9-bacteria	This study
DSL-D3 Δ <i>iclR</i> Δ <i>sdhA</i>	DSL Δ <i>iclR</i> Δ <i>sdhA</i> /pK-hemA-hemB/pgRNA-D3/pdcas9-bacteria	This study
DSL-D4 Δ <i>iclR</i> Δ <i>sdhA</i>	DSL Δ <i>iclR</i> Δ <i>sdhA</i> /pK-hemA-hemB/pgRNA-D4/pdcas9-bacteria	This study
DSL-D5 Δ <i>iclR</i> Δ <i>sdhA</i>	DSL Δ <i>iclR</i> Δ <i>sdhA</i> /pK-hemA-hemB/pgRNA-D5/pdcas9-bacteria	This study
DSL-D6 Δ <i>iclR</i> Δ <i>sdhA</i>	DSL Δ <i>iclR</i> Δ <i>sdhA</i> /pK-hemA-hemB/pgRNA-D6/pdcas9-bacteria	This study
DSL-D7 Δ <i>iclR</i> Δ <i>sdhA</i>	DSL Δ <i>iclR</i> Δ <i>sdhA</i> /pK-hemA-hemB/pgRNA-D7/pdcas9-bacteria	This study
DSL-D8 Δ <i>iclR</i> Δ <i>sdhA</i>	DSL Δ <i>iclR</i> Δ <i>sdhA</i> /pK-hemA-hemB/pgRNA-D8/pdcas9-bacteria	This study
DSL-D9 Δ <i>iclR</i> Δ <i>sdhA</i>	DSL Δ <i>iclR</i> Δ <i>sdhA</i> /pK-hemA-hemB/pgRNA-D9/pdcas9-bacteria	This study
Plasmids		
pCP20	Flp+, λ cI857+, λ pR Rep(pSC101 ori)ts, ApR, CmR	(Cherepanov & Wackernagel, 1995)
pK184	p15A ori, KmR, <i>Plac</i> :: <i>lacZ</i> '	(Jobling & Holmes, 1990)
pdcas9-bacteria	p15A ori, P _{Tet} -dCas9	(Qi et al., 2013)
pgRNA-bacteria	ColE1 origin, P _{J23119} -gRNA	(Qi et al., 2013)
pgRNA-D1	Derived from pgRNA-bacteria, P _{speI} :: <i>hemC</i> -gRNA-D1	This study
pgRNA-D2	Derived from pgRNA-bacteria, P _{speI} :: <i>hemC</i> -gRNA-D2	This study
pgRNA-D3	Derived from pgRNA-bacteria, P _{speI} :: <i>hemC</i> -gRNA-D3	This study
pgRNA-D4	Derived from pgRNA-bacteria, P _{speI} :: <i>hemC</i> -gRNA-D4	This study
pgRNA-D5	Derived from pgRNA-bacteria, P _{speI} :: <i>hemC</i> -gRNA-D5	This study
pgRNA-D6	Derived from pgRNA-bacteria, P _{speI} :: <i>hemC</i> -gRNA-D6	This study
pgRNA-D7	Derived from pgRNA-bacteria, P _{speI} :: <i>hemC</i> -gRNA-D7	This study
pgRNA-D8	Derived from pgRNA-bacteria, P _{speI} :: <i>hemC</i> -gRNA-D8	This study
pgRNA-D9	Derived from pgRNA-bacteria, P _{speI} :: <i>hemC</i> -gRNA-D9	This study
pK-hemA	Derived from pK184, <i>Plac</i> :: <i>hemA</i>	(Miscevic et al., 2021)
pK-hemA-hemB	Derived from pK184, <i>Plac</i> :: <i>hemA-hemB</i>	This study

3.2 Media and bacterial cell cultivation

All medium components were obtained from Sigma-Aldrich Co. (St Louis, MO, USA) except yeast extract and tryptone which were obtained from BD Diagnostic Systems (Franklin Lakes, NJ, USA). *E. coli* strains, stored as glycerol stocks at -80°C , were streaked on lysogeny broth (LB; 10 g L^{-1} tryptone, 5 g L^{-1} yeast extract, and 5 g L^{-1} NaCl) agar plates with appropriate antibiotics [ampicillin (100 mg L^{-1}), kanamycin (50 mg L^{-1}), and chloramphenicol (25 mg L^{-1})] and incubated at 37°C for 14-16 h.

For shake-flask cultivations, single colonies were picked from LB plates to inoculate 30 mL LB medium in 125 mL conical flasks. The cultures were shaken at 37°C and 280 rpm in a rotary shaker (New Brunswick Scientific, NJ, USA) and used as seed cultures to inoculate 220 mL LB media at 1% (v/v) in 1 L conical flasks with appropriate antibiotics. This second seed culture was shaken at 37°C and 280 rpm until the cell density reached 0.80 OD₆₀₀. Cells were then harvested by centrifugation at $9,000\times g$ and 20°C for 10 minutes and resuspended in 30 mL modified M9 production medium. The suspended culture was transferred into 125 mL screwed cap plastic flasks for shaking at 37°C at 280 rpm in a rotary shaker. Unless otherwise specified, the modified M9 production medium contained 25 g L^{-1} glycerol, 5 g L^{-1} yeast extract, 10 mM NaHCO_3 , 1 mM MgCl_2 , 200 mL L^{-1} of M9 salts mix (33.9 g L^{-1} Na_2HPO_4 , 15 g L^{-1} KH_2PO_4 , 5 g L^{-1} NH_4Cl , 2.5 g L^{-1} NaCl), 1 mL L^{-1} dilution of Trace Metal Mix A5 (2.86 g L^{-1} H_3BO_3 , 1.81 g L^{-1} $\text{MnCl}_2\cdot 4\text{H}_2\text{O}$, 0.222 g L^{-1} $\text{ZnSO}_4\cdot 7\text{H}_2\text{O}$, 0.39 g L^{-1} $\text{Na}_2\text{MoO}_4\cdot 2\text{H}_2\text{O}$, $79\text{ }\mu\text{g L}^{-1}$ $\text{CuSO}_4\cdot 5\text{H}_2\text{O}$, $49.4\text{ }\mu\text{g L}^{-1}$ $\text{Co}(\text{NO}_3)_2\cdot 6\text{H}_2\text{O}$), and was supplemented with 0.1 mM isopropyl β -D-1-thiogalactopyranoside (IPTG).

For bioreactor cultivation, single colonies were picked from LB plates to inoculate 30 mL super broth (SB) medium (32 g L^{-1} tryptone, 20 g L^{-1} yeast extract, and 5 g L^{-1} NaCl) in 125 mL

conical flasks. The overnight cultures were shaken at 37°C and 280 rpm in a rotary shaker (New Brunswick Scientific, NJ, USA) and used as seed cultures to inoculate 220 mL SB media at 1% (v/v) in 1 L conical flasks with appropriate antibiotics. This second seed cultures were shaken at 37°C and 280 rpm for 14-16 hours. Cells were then harvested by centrifugation at 9,000×g and 20°C for 10 minutes and resuspended in 50 mL fresh LB media. The suspended culture was used to inoculate a 1 L stirred tank bioreactor (containing two Rushton radial flow disks as impellers) (CelliGen 115, Eppendorf AG, Hamburg, Germany) at 37°C and 430 rpm. The semi-defined production medium in the batch bioreactor contained 30 g L⁻¹ glycerol, 0.23 g L⁻¹ K₂HPO₄, 0.51 g L⁻¹ NH₄Cl, 49.8 mg L⁻¹ MgCl₂, 48.1 mg L⁻¹ K₂SO₄, 1.52 mg L⁻¹ FeSO₄, 0.055 mg L⁻¹ CaCl₂, 2.93 g L⁻¹ NaCl, 0.72 g L⁻¹ tricine, 10 g L⁻¹ yeast extract, 10 mM NaHCO₃, and 1 mL L⁻¹ trace elements (2.86 g L⁻¹ H₃BO₃, 1.81 g L⁻¹ MnCl₂• 4H₂O, 0.222 g L⁻¹ ZnSO₄• 7H₂O, 0.39 g L⁻¹ Na₂MoO₄• 2H₂O, 79 µg L⁻¹ CuSO₄• 5H₂O, 49.4 µg L⁻¹ Co(NO₃)₂• 6H₂O) (Neidhardt et al., 1974), and was supplemented with 0.1 mM isopropyl β-D-1-thiogalactopyranoside (IPTG). Aerobic and microaerobic conditions were maintained by purging air into the bulk culture at 1 vvm and into the headspace at 0.1 vvm, respectively. The pH of the media was maintained at 7.0 ± 0.1 with 30% (v/v) NH₄OH and 15% (v/v) H₃PO₄ throughout the bioreactor cultivation.

3.3 Analysis

Culture samples were diluted with 0.15 M saline solution for measuring cell density in OD₆₀₀ using a spectrophotometer (DU520, Beckman Coulter, Fullerton, CA). Cell-free medium (Table S3) was prepared by centrifugation of the culture sample at 9,000×g for 5 minutes and filter sterilization using a 0.2 µm syringe filter. The quantification of extracellular metabolites and glycerol was conducted using high-performance liquid chromatography (HPLC) (LC-10AT, Shimadzu, Kyoto,

Japan) with a refractive index detector (RID; RID-10A, Shimadzu, Kyoto, Japan) and a chromatographic column (Aminex HPX-87H, Bio-Rad Laboratories, CA, USA). The HPLC column temperature was maintained at 35°C and the mobile phase was 5 mM H₂SO₄ (pH 2) running at 0.6 mL min⁻¹. The RID signal was acquired and processed by a data processing unit (Clarity Lite, DataApex, Prague, Czech Republic).

PBG titer in the cell-free medium was measured using a regular Ehrlich's reagent and PBG was colorimetrically quantified by taking a absorbance reading at 555 nm (Mauzerall & Granick, 1956). The percentage yield of PBG was defined as the mole ratio of the produced PBG to the theoretically maximal PBG produced based on the consumed glycerol with a molar ratio of one-to-six (i.e., one-mole PBG is derived from six-mole glycerol). Note that one-mole succinyl-CoA (derived from two-mole glycerol) and one-mole glycine (derived from one-mole glycerol) generate one-mole 5-ALA, whereas two-mole 5-ALA forms one-mole PBG. The bulk level of porphyrin compounds in the cell-free medium was estimated using a spectrophotometer at two specific wavelengths, i.e., 405 nm (measuring Soret band) and 495 nm (measuring Q-band). Note that all bioreactor cultivation results shown in this study were respectively obtained from a single batch run, with most of cultivation batches being duplicated or even triplicated to ensure their data reproducibility.

3.4 Real-time quantitative reverse transcription PCR (qRT-PCR)

For RNA extraction, *E. coli* cells were cultivated in 30 mL liquid LB medium at 37°C and harvested in the exponential growth phase. Total RNA isolation was done using the High Pure RNA Isolation Kit (Roche Diagnostics, Basel, Switzerland) as per manufacturer's instructions and stored at -80°C for later analysis. Complementary DNAs (cDNAs) were synthesized from 100 ng

of total RNA using the High-Capacity cDNA Reverse Transcription Kit (ThermoFisher Scientific, MA). Sequence-specific primers for *hemC* cDNA (i.e., q-hemC) and internal control *rrsA* (encoding ribosomal RNA 16S) cDNA (i.e., q-rrsA) were used for real-time PCR amplification in 25 μ L reaction mixture. Real-time qRT-PCR was carried out using the Power SYBR® Green PCR Master Mix (ThermoFisher Scientific; MA) in an Applied Biosystems StepOnePlus™ System as per the manufacturer's instructions. All quantification experiments were performed in duplicate.

3.5 Statistical analysis

All experimental data in this study were collected in duplicate for statistical analysis. In addition, data comparison was statistically analyzed with an unpaired two-tail Student's *t*-test based on 95% confidence level to ensure its statistical significance (Table S4). Hence, $P < 0.05$ was used as a standard criterion of statistical significance when comparing the means of experimental data, such as PBG titer.

Chapter 4

Results

4.1 Shake-flask cultivation for PBG bioproduction

The Shemin/C4 pathway was implemented in *E. coli* via heterologous expression of *hemA* from *R. sphaeroides* in BW Δ *ldhA* (Miscevic et al., 2021). The effects of implemented Shemin pathway were observed by comparing the native BW Δ *ldhA* *E. coli* strain and the resultant control strain, DMH, in screw-cap shake-flasks cultivation experiment with ~ 25 g L⁻¹ of glycerol as the carbon source. While BW Δ *ldhA* produced no detectable levels of PBG or porphyrin, DMH showed considerable porphyrin biosynthesis (Figure 5), suggesting the active Shemin pathway. The dark red color pigmentation of the DMH culture (Figure 5) suggests that a substantial amount of glycerol was converted to porphyrin pigments but with minimal PBG accumulation.

To prevent PBG intracellular conversion into HMB and then towards porphyrin formation, gene knockout of *hemC* would result in detrimental effects on cell physiology as *hemC* is an essential gene for heme synthesis and cell survival. Alternatively, CRISPRi was applied by designing four *hemC*-targeting gRNAs with different relative expression efficiencies (as predicted by the Chop-Chop online tool), generating four corresponding strains of DMH-D1, DMH-D2, DMH-D3, and DMH-D4 (Figure 5) (Table S2). Here, DMH-CT is the control strain without any *hemC*-targeting gRNA. Additionally, DMH-D4 Δ *iclR* Δ *sdhA* was tested to evaluate the effect of carbon flux direction from TCA cycle. Compared to DMH strain, the cell growth was minimally affected for other compared strains but some noticeable effect of reduced glycerol consumption in *hemC*-repressed strains, excluding DMH-D3, was observed. The low titers for produced acetate in control strains, DMH and DMH-CT, was due to complete consumption of glycerol before experiment

completion and acetate consumption follows. The reduction in degree of pigmentation in all *hemC*-repressed strains is supporting evidence for reduced carbon flux direction towards porphyrin formation due to CRISPRi effect. It was noticed that all these strains failed to produce significant amounts of PBG in shake flask cultivation with titers in range of few milligrams.

To enhance PBG biosynthesis and accumulation, we cloned the native *hemB* gene from *E. coli* for heterologous expression along with *hemA* from *R. sphaeroides*, resulting in another control strain DSL and other derived strains, including different set of *hemC*-repressed strains. Some effective on cell growth was observed for *hemC*-repressed strains, except for DSL-D4 Δ *iclR* Δ *sdhA*, but no appreciable improvement in overall PBG titers was observed.

Consequently, strain characterization studies with bioreactor fermentation were designed for testing in aerobic and microaerobic conditions and new gRNAs (along with previously designed set of four gRNAs) were explored for improved PBG titers and reduced carbon flux direction towards porphyrin synthesis.

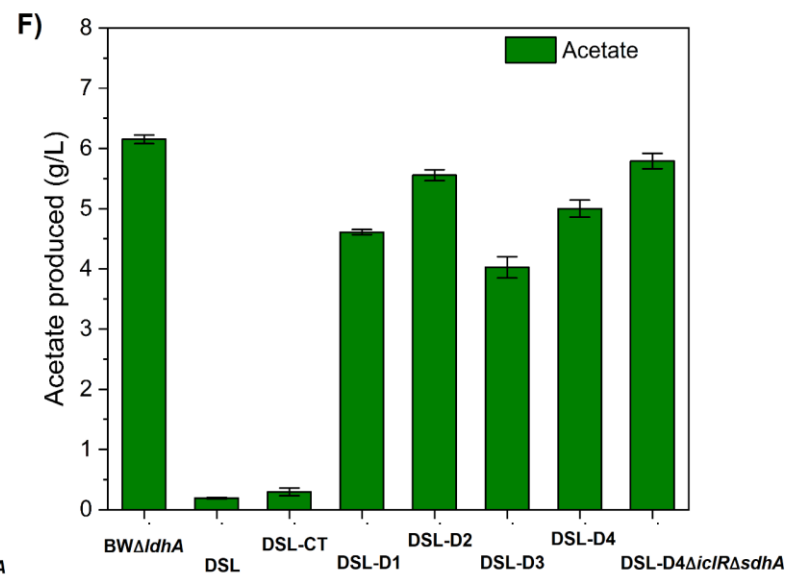
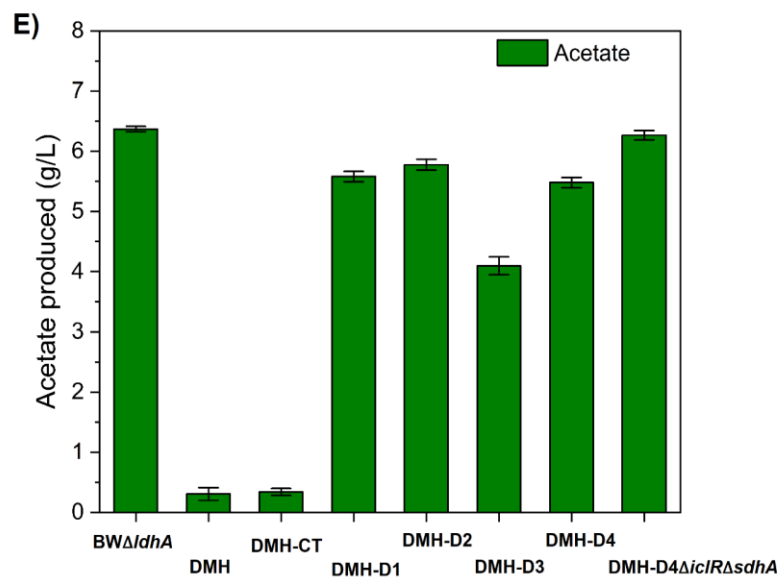
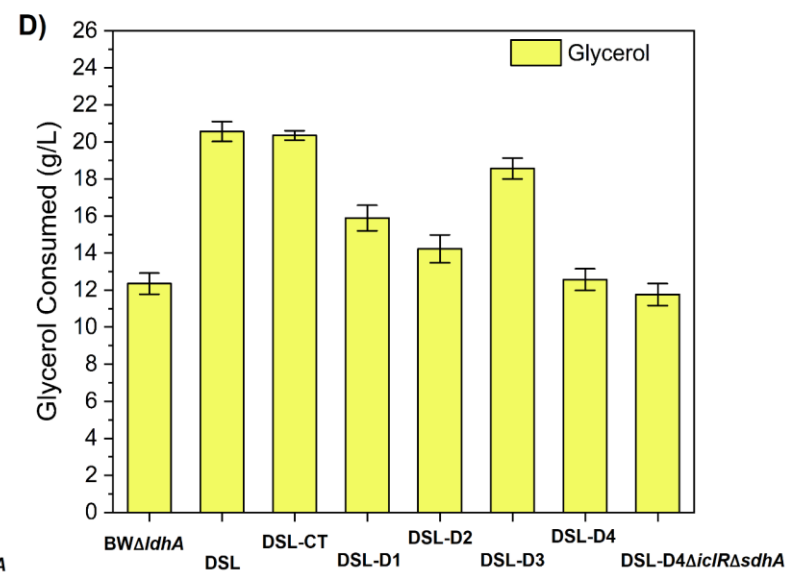
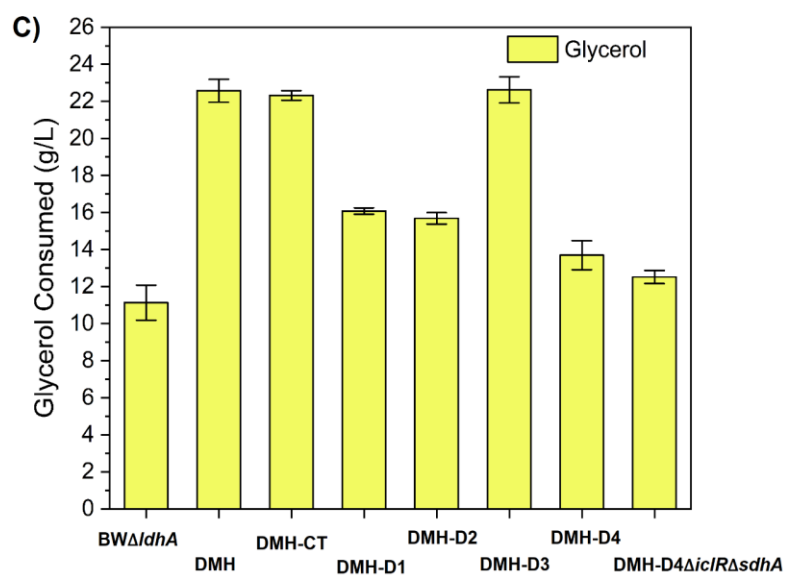
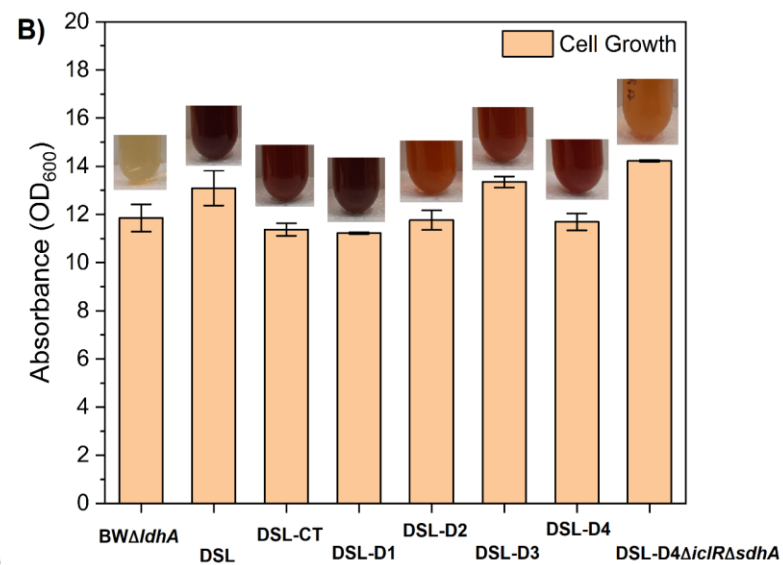
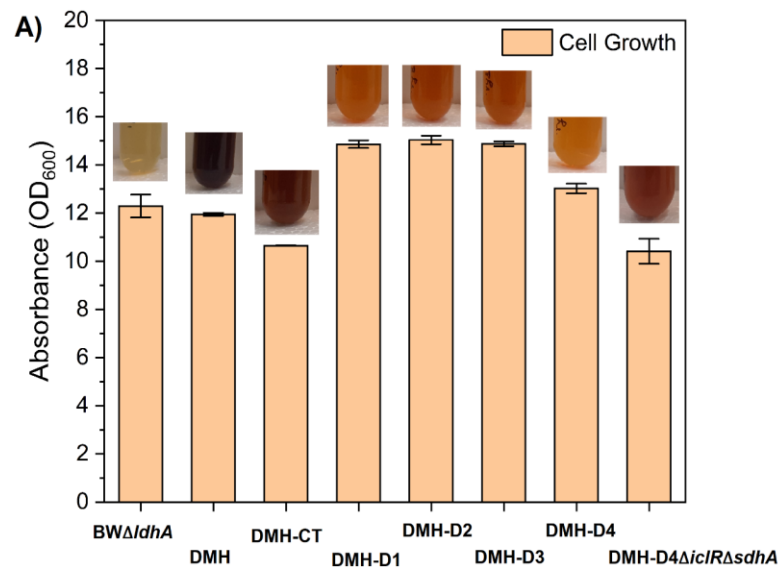


Figure 5. Shake flask cultivation of BW Δ *ldhA*, DMH, DSL and other derived *hemC*-repressed strains for PBG extracellular accumulation. Comparison results shown for 48 hr. shake-flask cultivation include A) cell density (OD600) with the images of final cell-free media sample, C) glycerol consumption, and E) acetate titers for strains: BW Δ *ldhA*, DMH, DMH-CT, DMH-D1, DMH-D2, DMH-D3, DMH-D4, and DMH-D4 Δ *iclR* Δ *sdhA*. Other results shown for 48 hr. shake-flask cultivation include B) cell density (OD600) with the images of final cell-free media sample, C) glycerol consumption, and E) acetate titers compared for for strains: BW Δ *ldhA*, DSL, DSL-CT, DSL-D1, DSL-D2, DSL-D3, DSL-D4, and DSL-D4 Δ *iclR* Δ *sdhA*. All values are reported as means \pm SD (n = 2).

4.2 Carbon flux direction from the TCA pathways to the Shemin/C4 pathway

The control strain, DMH, was cultivated under aerobic conditions in a batch bioreactor with \sim 30 g L⁻¹ of glycerol as the carbon source. The supply of excess oxygen supported cell growth with effective glycerol consumption, resulting in 120 mg L⁻¹ of the peak PBG titer (1.31% yield) with substantial acetate formation (69.3% yield) (Figure 6). Extending the cultivation, based on the remaining glycerol, and produced acetate, resulted in reduction of PBG titer to 75.1 mg L⁻¹ (0.65% yield) with increased porphyrin formation. While the formation of other byproduct metabolites, such as ethanol, succinate, and formate, was minimal, the results suggest the need for metabolic strategies to reduce carbon flux drainage toward acetogenesis and porphyrin biosynthesis for enhanced PBG accumulation.

PBG biosynthesis via the C4 pathway utilizes succinyl-CoA as a key precursor (with the other being glycine) to produce 5-ALA as an intermediate before subsequent conversion to PBG.

The intracellular succinyl-CoA supply is affected by three oxygen-sensitive metabolic routes associated with the central metabolism, i.e., oxidative TCA cycle, reductive TCA branch, and glyoxylate shunt (Figure 1). Due to more effective cell growth and glycerol consumption, we first characterized our engineered strains under aerobic conditions. To direct more carbon flux toward the succinyl-CoA node, we inactivate the oxidative TCA cycle by knocking out the *sdhA* gene, resulting in the mutant strain DMH Δ *sdhA*, with an improved peak PBG titer of 154 mg L⁻¹ (1.41% yield) and 115 mg L⁻¹ (1.01% yield) at the end of bioreactor cultivation (Figure 6). On the other hand, we also deregulated glyoxylate shunt by knocking out the *iclR* gene, resulting in the mutant strain DMH Δ *iclR* in which more carbon flux could be directed toward the succinyl-CoA node via glyoxylate shunt with reduced decarboxylation through bypassing the oxidative TCA cycle. Aerobic bioreactor cultivation of DMH Δ *iclR* also showed improved peak PBG titer of 130 mg L⁻¹ (1.13% yield) and 80.7 mg L⁻¹ (0.69% yield) at the end of the cultivation (Figure 6). Both single-mutant strains of DMH Δ *iclR* and DMH Δ *sdhA* displayed effective cell growth and glycerol consumption, with reduced acetate production (32.1% and 38.0% yield, respectively) compared to control strain DMH.

Next, we derived the double mutant strain DMH Δ *iclR* Δ *sdhA* such that the carbon flux from the deregulated glyoxylate shunt could be further directed toward the succinyl-CoA node via the reductive TCA branch for enhanced biosynthesis of PBG and porphyrins while minimizing decarboxylation. Aerobic bioreactor cultivation of DMH Δ *iclR* Δ *sdhA* produced 87.3 mg L⁻¹ (0.66% yield) at the end of cultivation (Figure 7). Moreover, we observed significantly reduced acetate formation with 35.9% yield, compared to the control strain DMH. These results indicate successful carbon flux direction from the TCA pathways to the C4 pathway in DMH Δ *iclR* Δ *sdhA*. However, the directed carbon flux appeared to proceed toward porphyrin formation rather than PBG

accumulation in these engineered strains, as indicated by subsequent reduction in PBG titer after reaching a peak value. While blocking the conversion of PBG to HMB by knocking out *hemC* appears to be a feasible way to promote PBG accumulation, such gene knockout is lethal due to physiological requirement of essential porphyrins.

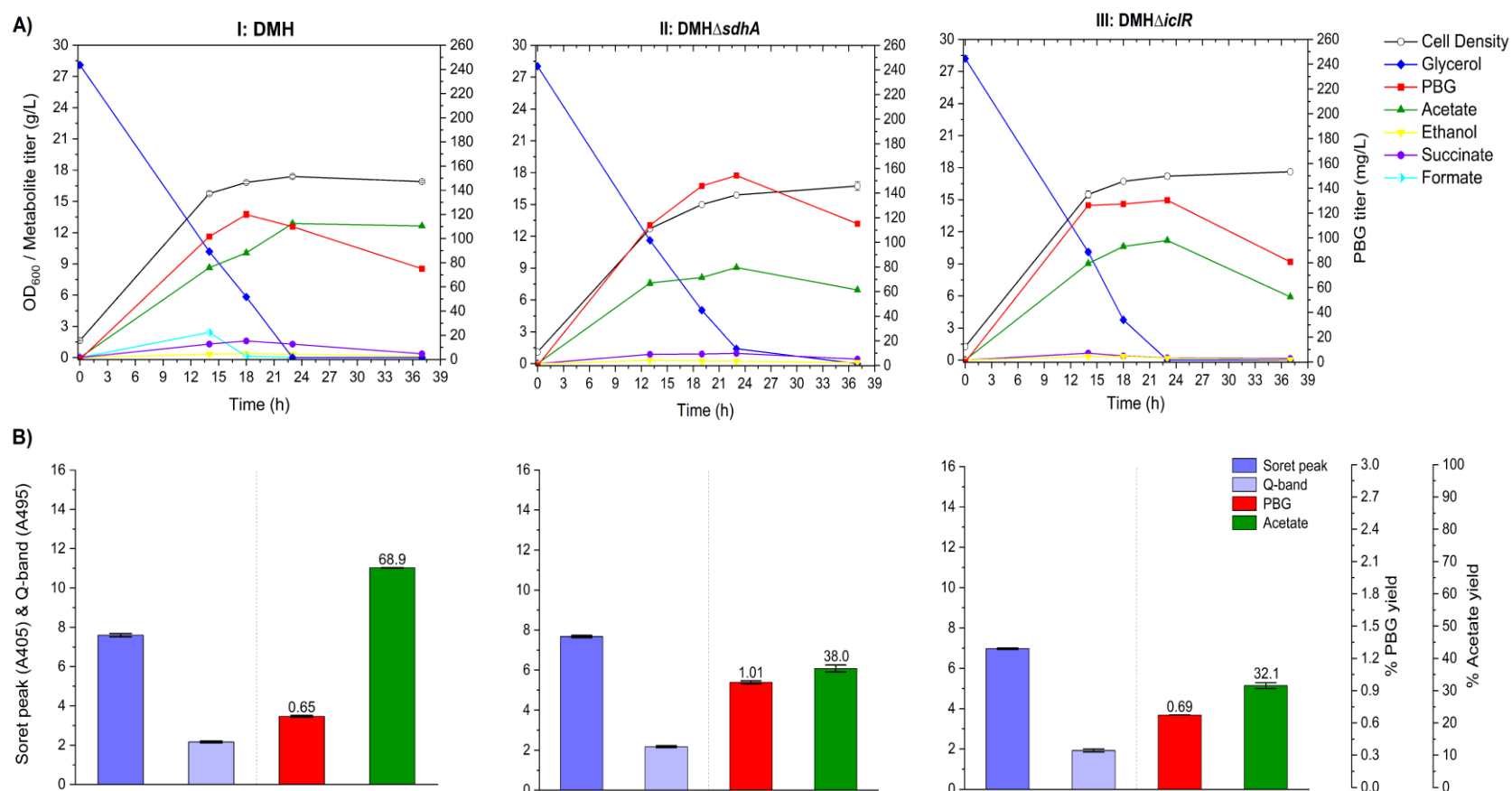


Figure 6. Bioreactor cultivation of DMH, DMH Δ *sdhA*, and DMH Δ *iclR* for PBG biosynthesis under aerobic conditions. Time profiles of cell density (OD₆₀₀), glycerol consumption and metabolite production profiles, acetate and PBG percentage yields, and extracellular accumulation of porphyrins (represented by the absorbance readings of the Soret peak (A405) and Q-band (A495)) are shown. The percentage yields of acetate/PBG and absorbance readings of porphyrin compounds are calculated/measured based on the consumed glycerol at end of cultivation. **(I)** DMH, **(II)** DMH Δ *sdhA*, **(III)** DMH Δ *iclR*. All values are reported as means \pm SD (n = 2).

4.3 Repression of *hemC* expression for PBG biosynthesis and accumulation

Since *hemC* is an essential gene, gene knockdown to repress *hemC* expression was explored to promote PBG accumulation with minimal impact on cell physiology and PBG biosynthesis. Hence, CRISPRi was applied using *hemC*-targeting gRNAs with distinct expression efficiencies (predicted by CHOPCHOP). Upon first screening of a selection of gRNAs targeting different areas of *hemC* (Figure 4; Table S2) based on bioreactor cultivation, *hemC*-gRNA-D9 appeared to show effective *hemC* repression with enhanced PBG biosynthesis and accumulation. The *hemC*-repression effect was further verified by qRT-PCR (Figure 12). Hence, the resulting *hemC*-repressed strains based on the use of *hemC*-gRNA-D9 were selected for complete bioreactor characterization. Under aerobic bioreactor conditions, cell growth and glycerol utilization for DMH-D9 Δ *iclR* Δ *sdhA* were minimally affected compared to the control strain DMH Δ *iclR* Δ *sdhA*, suggesting that the need of essential porphyrins for cell survival was properly met in the presence of *hemC* repression. Importantly, we observed more effective biosynthesis and accumulation of PBG, achieving a peak/final titer of 140 mg L⁻¹ (1.22% yield) at the end of the cultivation (Figure 7). Note that the Soret peak and Q-band absorbance values of the cell-free medium for the culture sample of DMH-D9 Δ *iclR* Δ *sdhA* was reduced to some extent, suggesting successful *hemC* repression with reduced porphyrin formation.

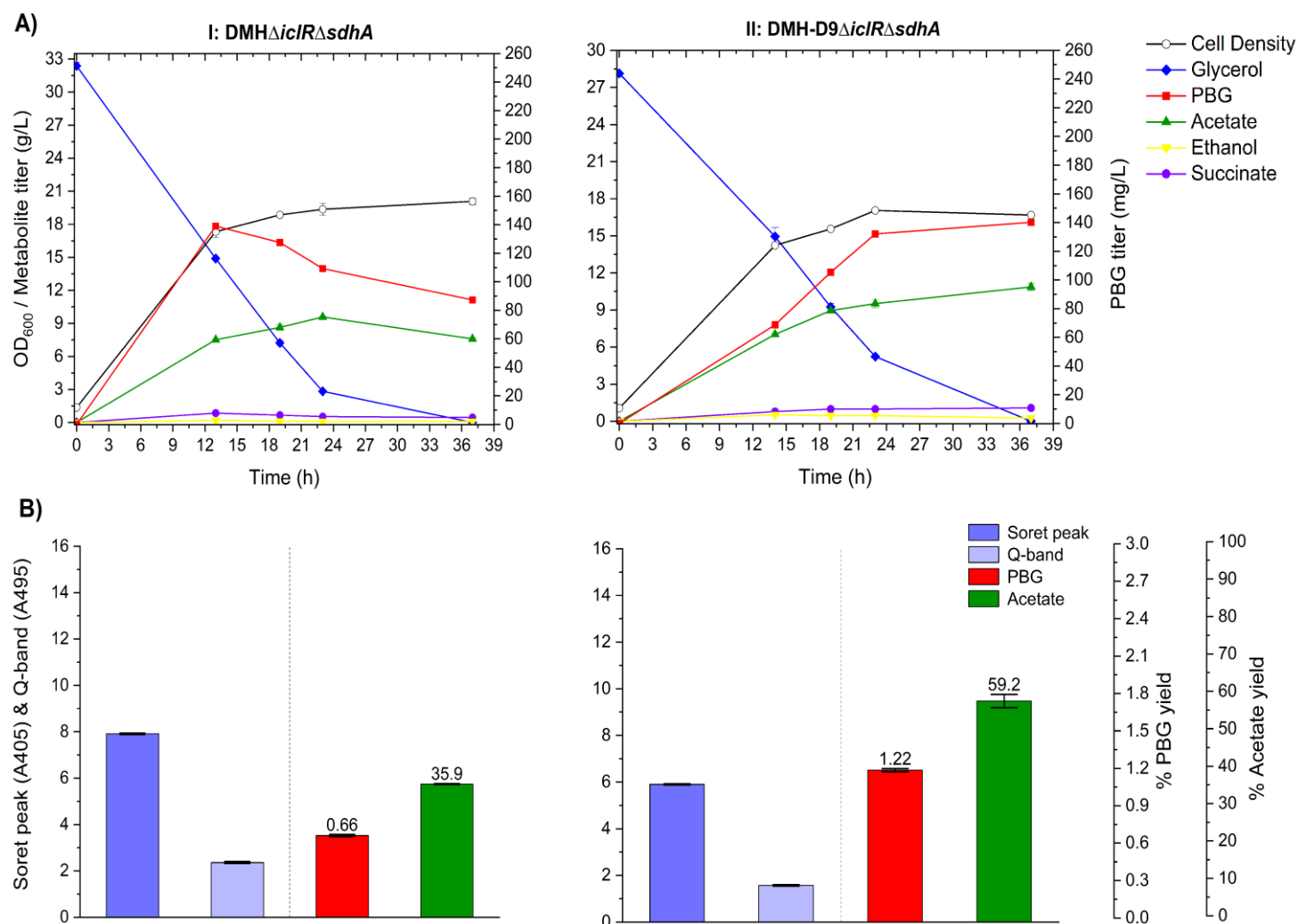


Figure 7. Bioreactor cultivation of DMH Δ iclR Δ sdhA and DMH-D9 Δ iclR Δ sdhA for PBG biosynthesis under aerobic conditions.

Time profiles of cell density (OD₆₀₀), glycerol consumption and metabolite production profiles, acetate and PBG percentage yields, and extracellular accumulation of porphyrins (represented by the absorbance readings of the Soret peak (A405) and Q-band (A495)) are shown. The percentage yields of acetate/PBG and absorbance readings of porphyrin compounds are calculated/measured based on the consumed glycerol at end of cultivation. Final PBG titer comparison for DMH, DMH Δ iclR Δ sdhA, and DMH-D9 Δ iclR Δ sdhA was deemed to be statistically significant (Table S4). **(I)** DMH Δ iclR Δ sdhA, **(II)** DMH-D9 Δ iclR Δ sdhA. All values are reported as means \pm SD (n = 2).

4.4 Increasing *hemB* expression to enhance PBG biosynthesis and accumulation

To further enhance PBG biosynthesis and accumulation, we cloned the native *hemB* gene from *E. coli* for heterologous expression along with *hemA* from *R. sphaeroides*, resulting in another control strain DSL. While aerobic bioreactor cultivation of DSL led to a much higher peak PBG titer compared to DMH, the PBG titer reduced rapidly upon extended cultivation to 65.7 mg L⁻¹ (0.52% yield) (Figure 8), a level similar to DMH. Porphyrin biosynthesis in DSL appeared to be higher than DMH, as evidenced by higher Soret peak and Q-band absorbance values of the cell-free medium for the culture sample. Also note that cell growth and glycerol consumption remained effective for DSL compared to DMH.

Similar to DMH, the metabolic limitations associated with excessive carbon flux drainage toward acetogenesis and porphyrin formation in DSL should be addressed. We derived single mutant strains of DSL Δ *sdhA* and DSL Δ *iclR* with the *sdhA* and *iclR* gene knockouts, respectively. While these single mutant strains didn't improve PBG biosynthesis significantly upon aerobic bioreactor cultivation, they showed metabolic effects similar to the corresponding DMH single mutant strains (Figure 8). We further derived the double mutant strain DSL Δ *iclR* Δ *sdhA*, which showed significantly enhanced PBG biosynthesis compared to the DSL control and single mutant strains upon aerobic bioreactor cultivation, i.e., a PBG titer of 104 mg L⁻¹ (0.81% yield) at the end of the cultivation (Figure 9). Moreover, reduced acetogenesis was observed in DSL Δ *iclR* Δ *sdhA* with effective glycerol utilization and cell growth, suggesting successful carbon flux direction towards the succinyl CoA node for PBG and porphyrin biosynthesis under this new genetic background.

Different gRNAs (D1, D2, D3, D4, D5, D6, D7, D8, and D9) (Table S2) were initially designed and tested experimentally in a bioreactor setup for accessing their effectiveness in enhancing PBG titer compared to the control strain, *DSLΔiclRΔsdhA* (Figure 9, 10, and 11). Based on these preliminary results, two gRNA candidates (D6 and D9) with superior culture performance were selected for further evaluation. Finally, D9-gRNA system was identified to outperform D6-gRNA under various genetic background and therefore was chosen for more complete characterization. The effectiveness of *hemC*-gRNA-D6 and *hemC*-gRNA-D9 in repression of *hemC* gene was also confirmed with qRT-PCR studies, where reduced levels of *hemC* gene expression was seen compared to control strain, *DSLΔiclRΔsdhA* (Figure 12)

Furthermore, aerobic bioreactor cultivation of *DSL-D9ΔiclRΔsdhA* showed much improved PBG biosynthesis and accumulation, i.e., a PBG titer at 209 mg L⁻¹ (1.73% yield) at the end of the cultivation, though glycerol consumption and cell growth were slightly affected. Note that the final PBG yield for *DSL-D9ΔiclRΔsdhA* was 2.14-fold that for the control *DSLΔiclRΔsdhA*, suggesting the effectiveness of *hemC* repression toward enhanced PBG biosynthesis and accumulation (Figure 9).

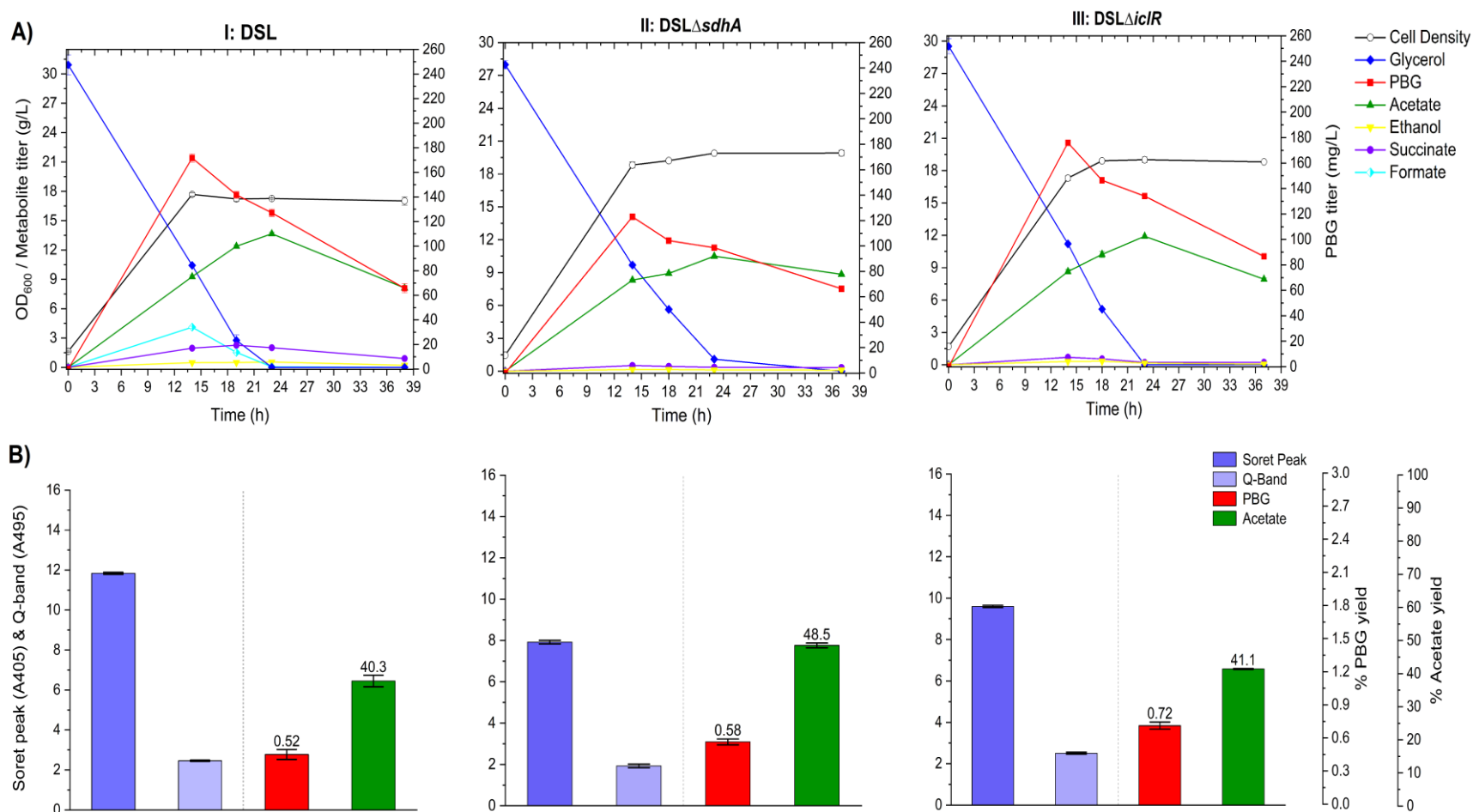


Figure 8. Bioreactor cultivation of DSL, DSL Δ *sdhA*, and DSL Δ *iclR* for PBG biosynthesis under aerobic conditions. Time profiles of cell density (OD₆₀₀), glycerol consumption and metabolite production profiles, acetate and PBG percentage yields, and extracellular accumulation of porphyrins (represented by the absorbance readings of the Soret peak (A405) and Q-band (A495)) are shown. The percentage yields of acetate/PBG and absorbance readings of porphyrin compounds are calculated/measured based on the consumed glycerol at end of cultivation. (I) DSL, (II) DSL Δ *sdhA*, (III) DSL Δ *iclR*. All values are reported as means \pm SD (n = 2).

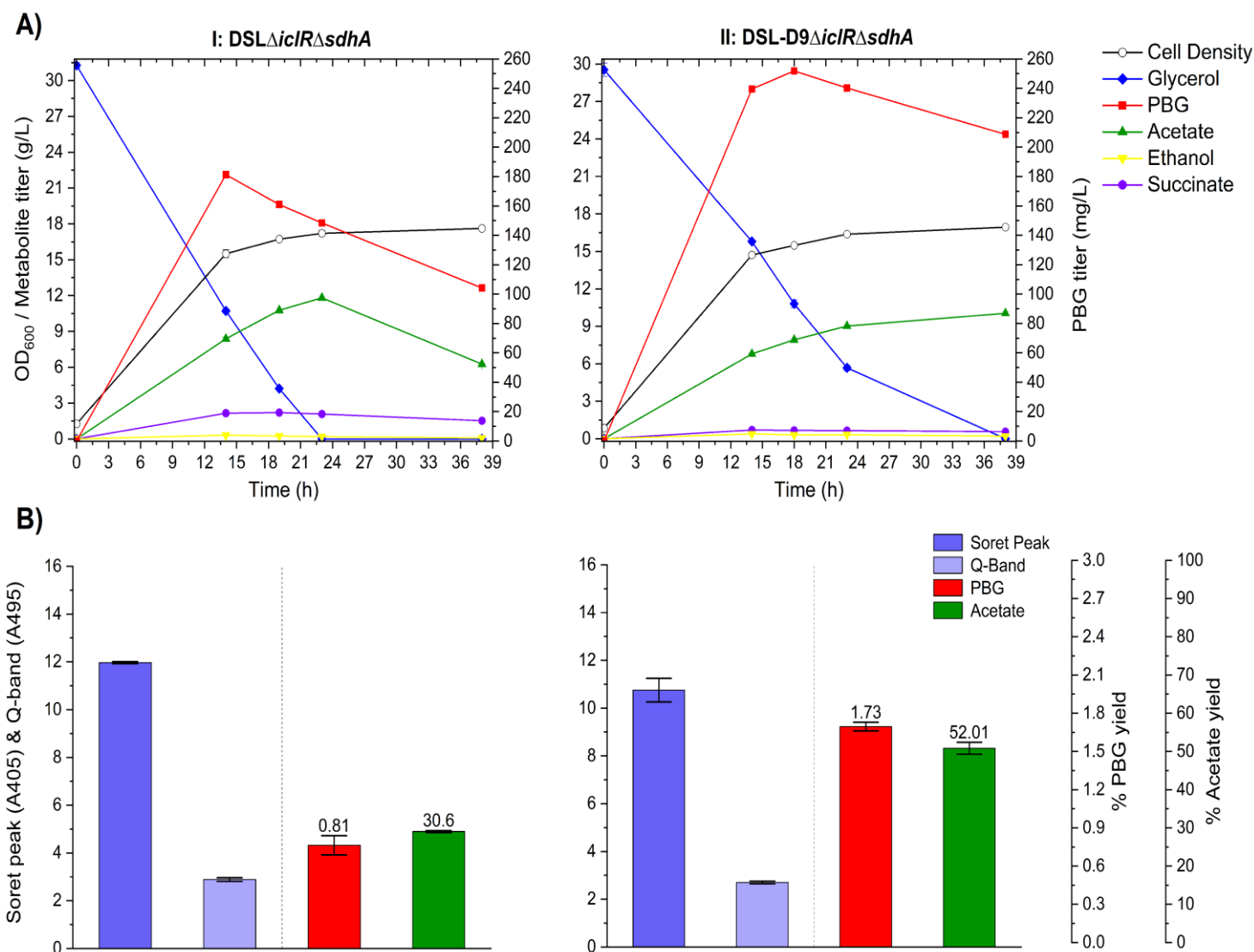


Figure 9. Bioreactor cultivation of DSL Δ iclR Δ sdhA and DSL-D9 Δ iclR Δ sdhA for PBG biosynthesis under aerobic conditions.

Time profiles of cell density (OD₆₀₀), glycerol consumption and metabolite production profiles, acetate and PBG percentage yields, and extracellular accumulation of porphyrins (represented by the absorbance readings of the Soret peak (A405) and Q-band (A495)) are shown. The percentage yields of acetate/PBG and absorbance readings of porphyrin compounds are calculated/measured based on the consumed glycerol at end of cultivation. Final PBG titer comparison for DSL, DSL Δ iclR Δ sdhA, and DSL-D9 Δ iclR Δ sdhA was deemed to be statistically significant (Table S4). **(I)** DSL Δ iclR Δ sdhA, **(II)** DSL-D9 Δ iclR Δ sdhA. All values are reported as means \pm SD (n = 2).

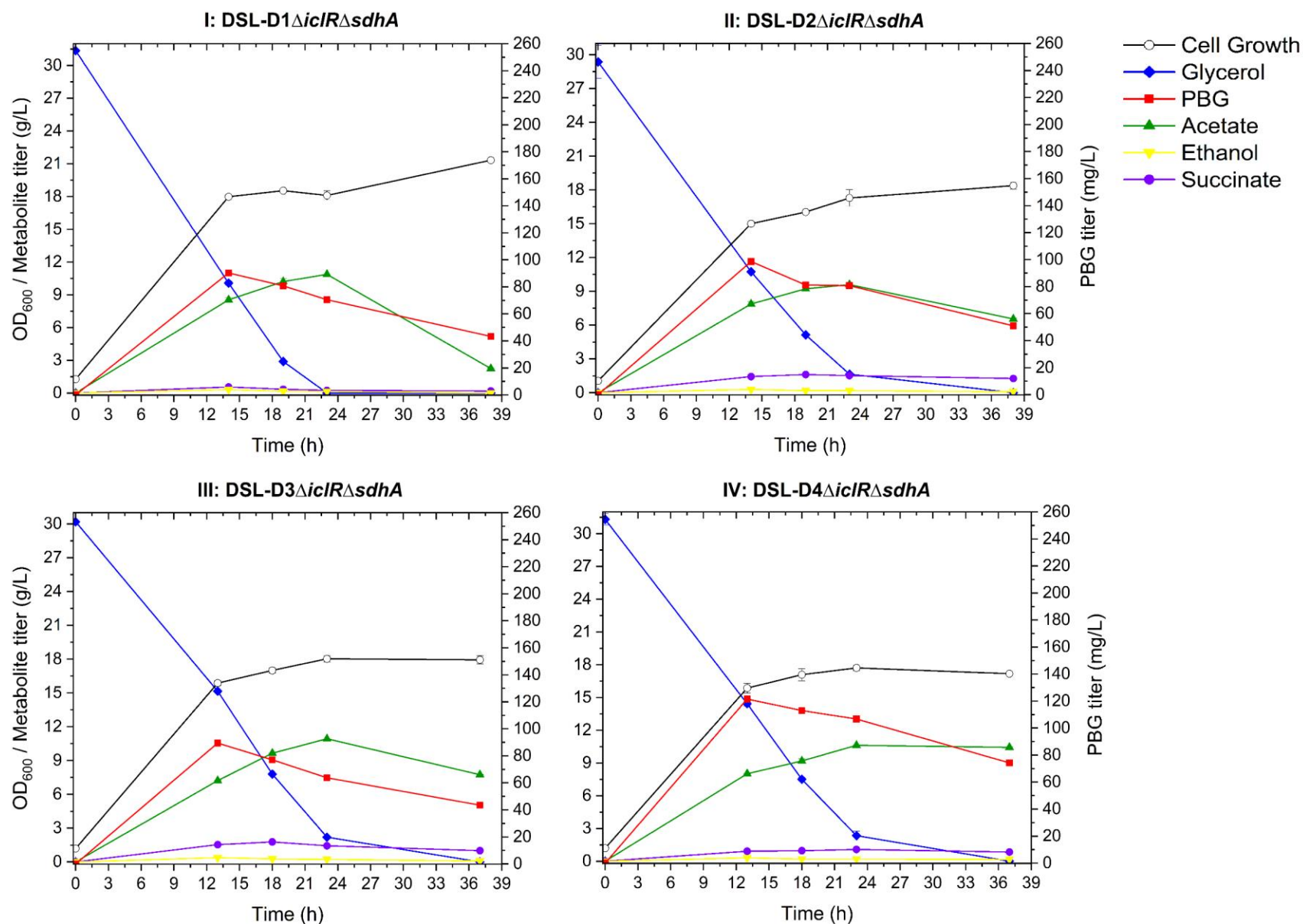


Figure 10. Bioreactor cultivation of DSL-D1Δ*iclR*Δ*sdhA*, DSL-D2Δ*iclR*Δ*sdhA*, DSL-D3Δ*iclR*Δ*sdhA*, and DSL-D4Δ*iclR*Δ*sdhA* for PBG biosynthesis under aerobic conditions. Time profiles of cell density (OD₆₀₀), glycerol consumption and metabolite extracellular accumulation profiles are shown. (I) DSL-D1Δ*iclR*Δ*sdhA*, (II) DSL-D2Δ*iclR*Δ*sdhA*, (III) DSL-D3Δ*iclR*Δ*sdhA*, (IV) DSL-D4Δ*iclR*Δ*sdhA*. All values are reported as means ± SD (n = 2).

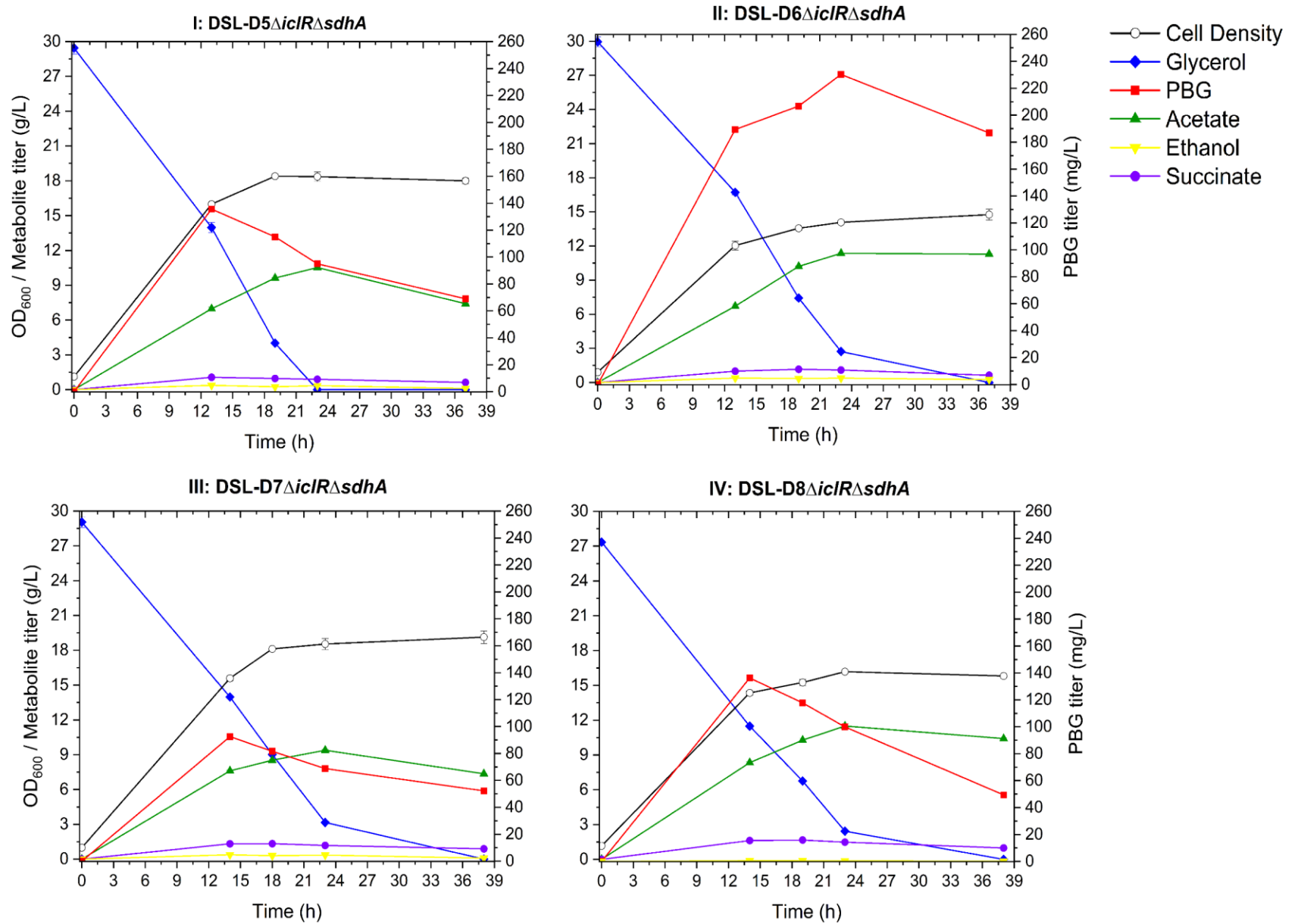


Figure 11. Bioreactor cultivation of DSL-D5Δ*iclR*Δ*sdhA*, DSL-D6Δ*iclR*Δ*sdhA*, DSL-D7Δ*iclR*Δ*sdhA*, and DSL-D8Δ*iclR*Δ*sdhA* for PBG biosynthesis under aerobic conditions. Time profiles of cell density (OD₆₀₀), glycerol consumption and metabolite extracellular accumulation profiles are shown. (I) DSL-D5Δ*iclR*Δ*sdhA*, (II) DSL-D6Δ*iclR*Δ*sdhA*, (III) DSL-D7Δ*iclR*Δ*sdhA*, (IV) DSL-D8Δ*iclR*Δ*sdhA*. All values are reported as means ± SD (n = 2).

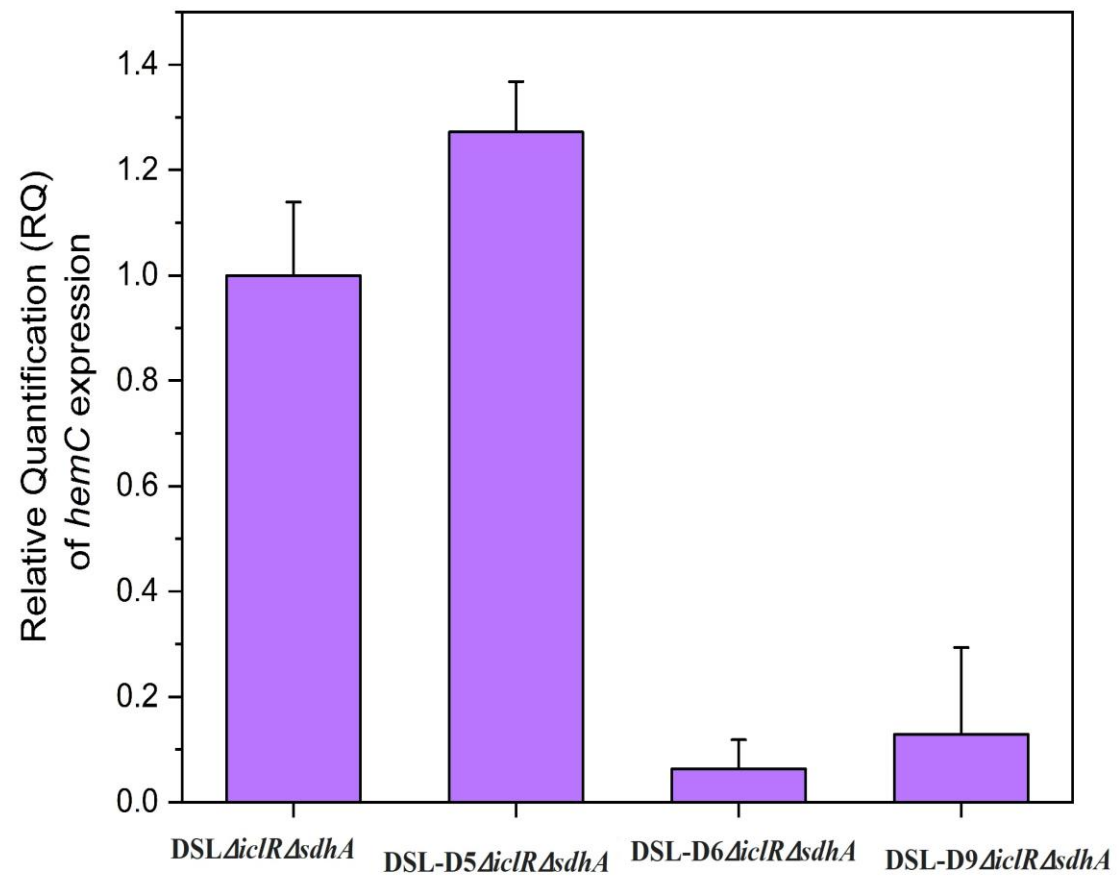


Figure 12. Quantification of the relative *hemC* expression for select gRNAs using qRT-PCR. All qRT-PCR values are reported as means \pm SD (n = 2).

4.5 Strain engineering for PBG biosynthesis under microaerobic conditions

Using engineered strains with the single *sdhA* mutation, we also explored PBG biosynthesis under oxygen-limited (i.e., microaerobic) conditions. Due to the inactivated oxidative TCA cycle with a regulated glyoxylate shunt, cell growth and glycerol utilization under microaerobic conditions for these control and mutant strains were ineffective compared to aerobic cultivation. In general, PBG biosynthesis under microaerobic conditions was also ineffective compared to aerobic cultivation. For the control strain DMH, the final PBG titer for microaerobic bioreactor cultivation was lower than that for aerobic cultivation, only reaching 48.7 mg L⁻¹ (0.41% yield) (Figure 13), with poor glycerol utilization and cell growth. Interestingly, porphyrin biosynthesis under microaerobic conditions appeared to be more effective, as evidenced by higher Soret peak and Q-band absorbance values, than aerobic cultivation. Compared to the control strain DMH, PBG biosynthesis under microaerobic conditions for the single mutant strain DMHΔ*sdhA*, in which only the reductive TCA branch was functional, was slightly improved, reaching a final PBG titer of 55.9 mg L⁻¹ (0.46% yield), with similar acetogenesis, cell growth, glycerol utilization, and porphyrin formation (Figure 13). We then evaluated the effects of *hemC* repression in DMH-D9Δ*sdhA* under microaerobic conditions and observed slightly better PBG biosynthesis, achieving a final PBG titer of 62.5 mg L⁻¹ (0.53% yield), with reduced porphyrin formation (Figure 13). Note that the peak PBG titers for DMH and DMHΔ*sdhA* cultivations were comparatively higher than that for DMH-D9Δ*sdhA*, implying PBG was rather unstable under such genetic backgrounds. Similar genetic and metabolic effects under microaerobic conditions described above in DMH single mutant strains were also observed in the corresponding DSL single mutant strains with higher *hemB* gene dosages. The final PBG titers for microaerobic bioreactor cultivation were 57.9, 67.2, and 83.8 mg L⁻¹ for DSL, DSLΔ*sdhA*, and DSL-D9Δ*sdhA*, respectively (Figure 14). Note

that the PBG yield for DSL-D9 Δ *sdhA* was only 1.16-fold that for DSL Δ *sdhA*, suggesting that the effect of *hemC* repression on PBG biosynthesis and accumulation was insignificant under microaerobic conditions.

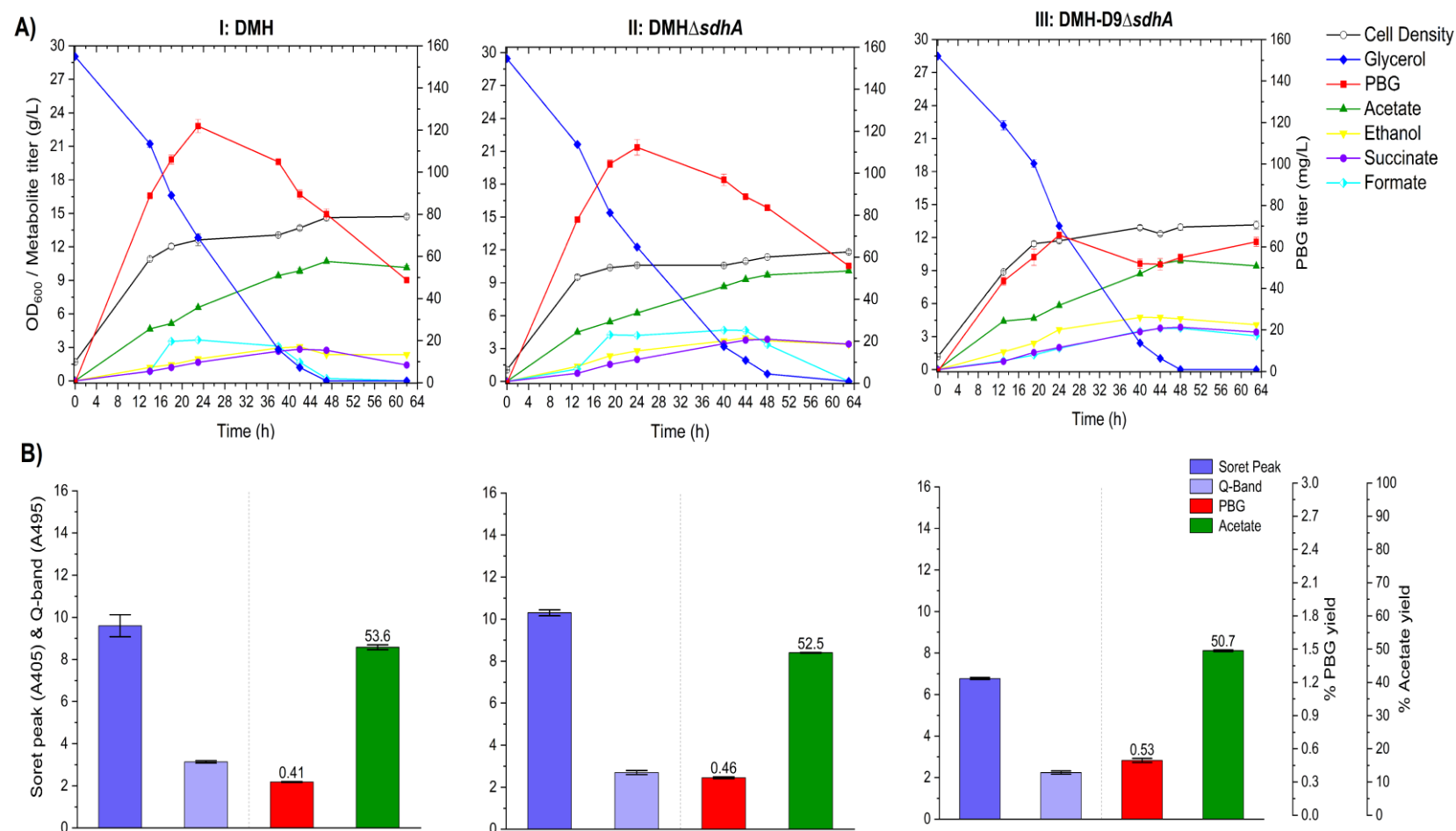


Figure 13. Bioreactor cultivation of DMH, DMH Δ *sdhA*, and DMH-D9 Δ *sdhA* for PBG biosynthesis under microaerobic conditions. Time profiles of cell density (OD₆₀₀), glycerol consumption and metabolite production profiles, acetate and PBG percentage yields, and extracellular accumulation of porphyrins (represented by the absorbance readings of the Soret peak (A405) and Q-band (A495)) are shown. The percentage yields of acetate/PBG and absorbance readings of porphyrin compounds are calculated/measured based on the consumed glycerol at end of cultivation. (I) DMH, (II) DMH Δ *sdhA*, (III) DMH-D9 Δ *sdhA*. All values are reported as means \pm SD (n = 2).

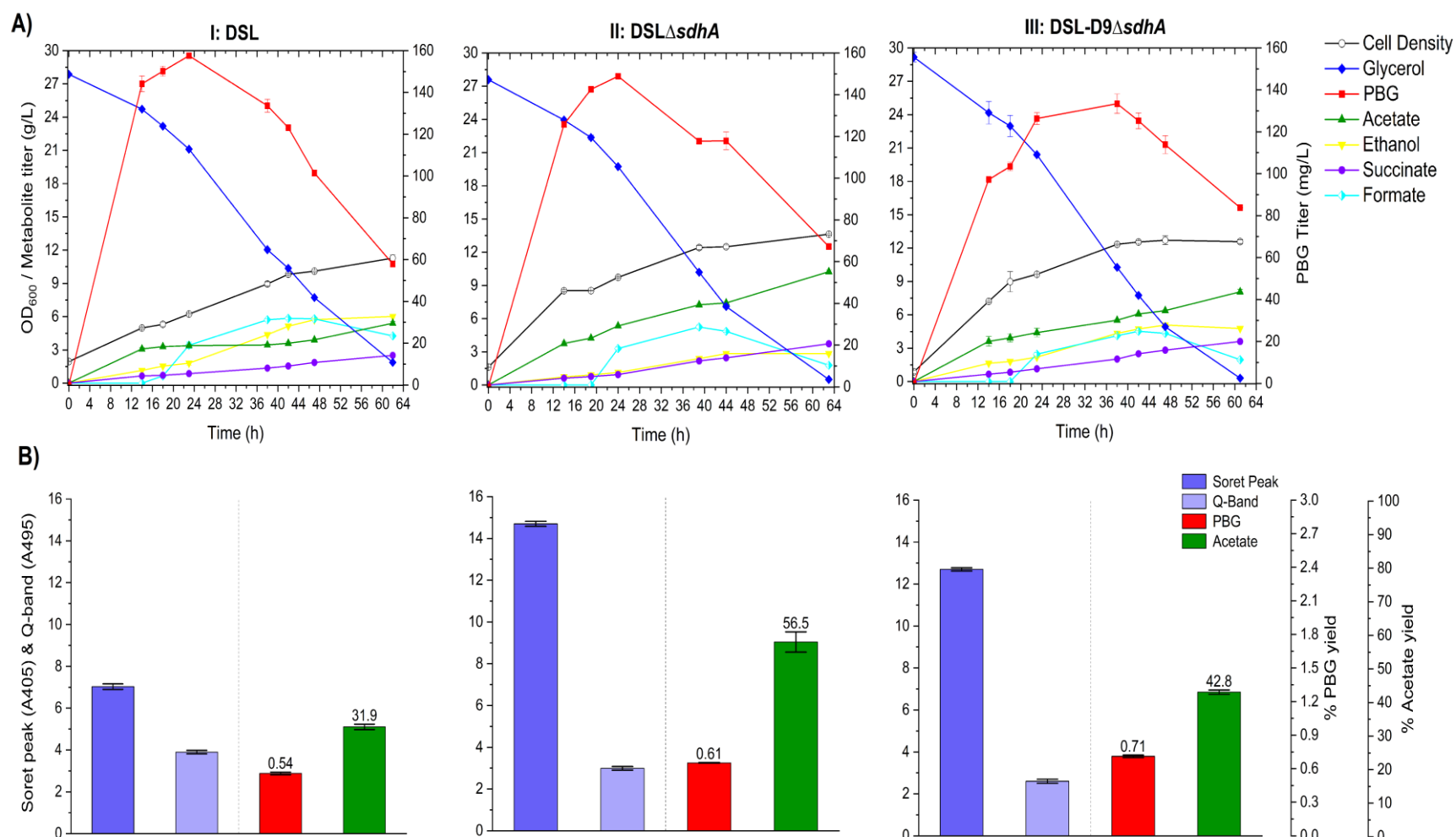


Figure 14. Bioreactor cultivation of DSL, DSL Δ *sdhA*, and DSL-D9 Δ *sdhA* for PBG biosynthesis under microaerobic conditions.

Time profiles of cell density (OD₆₀₀), glycerol consumption and metabolite production profiles, acetate and PBG percentage yields, and extracellular accumulation of porphyrins (represented by the absorbance readings of the Soret peak (A405) and Q-band (A495)) are shown. The percentage yields of acetate/PBG and absorbance readings of porphyrin compounds are calculated/measured based on the consumed glycerol at end of cultivation. Final PBG titer comparison for DSL, DSL Δ *sdhA*, and DSL-D9 Δ *sdhA* was deemed to be statistically significant (Table S4). (I) DSL, (II) DSL Δ *sdhA*, (III) DSL-D9 Δ *sdhA*. All values are reported as means \pm SD (n = 2)

Chapter 5

Discussion

As an intermediate in the metabolic pathway for essential porphyrin biosynthesis, PBG barely accumulates and, therefore, can be hardly detected in the extracellular medium upon cultivation of wild-type *E. coli*. In this study, we employed genetic and metabolic strategies for strain engineering of *E. coli* to enhance PBG biosynthesis for extracellular accumulation. First, the Shemin/C4 pathway was genetically implemented in *E. coli* by heterologous expression of *hemA* from *R. sphaeroides* to mediate molecular fusion of succinyl-CoA and glycine to form the key precursor 5-ALA for biosynthesis of PBG and porphyrins. Second, metabolic strategies were applied to direct carbon flux from the TCA pathways to the C4 pathway via the succinyl-CoA node. Third, the metabolic flux within the C4 pathway was further boosted by heterologous coexpression of *hemA* from *R. sphaeroides* and the native *E. coli hemB*. Finally, CRISPRi was applied to repress *hemC* expression to promote PBG accumulation with minimal impact to cell physiology and viability. PBG biosynthesis and accumulation in various engineered *E. coli* strains were characterized using bioreactor cultivation under different oxygenic (i.e., aerobic and microaerobic) conditions. Note that inclusion of episomal plasmids for heterologous expression of genes and implementing CRISPRi strategy in various engineered strains require constant use of antibiotic selection during cultivation, subsequently increasing the overall production cost.

Compared to the native *E. coli* in which porphyrin biosynthesis was primarily mediated via the C5 pathway, implementation of the heterologous C4 pathway significantly enhanced porphyrin biosynthesis based on visualization of high red-pigmentation upon bacterial cultivation (Table S3). Nevertheless, PBG titer remained low with significant carbon spill toward acetogenesis, as shown

in the control strain DMH cultivated under aerobic conditions. Since succinyl-CoA serves as a key precursor of the C4 pathway for biosynthesis of PBG and porphyrins, metabolic strategies were developed to increase this precursor supply. In *E. coli*, succinyl-CoA can be derived via three oxygen-dependent TCA pathways: (i) reductive TCA branch, (ii) oxidative TCA cycle, and (iii) glyoxylate shunt (Figure 1) (Cheng et al., 2013). In this study, we explored two metabolic routes for carbon flux direction toward succinyl-CoA within the TCA pathways, i.e., (i) deregulated glyoxylate shunt and reductive TCA branch via the double mutation of *iclR* and *sdhA* under aerobic conditions, and (ii) reductive TCA branch via the single mutation of *sdhA* under microaerobic conditions. Hence, the effects of individual single mutations and double mutation of *iclR* and *sdhA* on PBG biosynthesis were investigated.

Under aerobic conditions, biosynthesis of PBG and porphyrins was enhanced in DMH Δ *iclR* Δ *sdhA* compared to the control DMH, suggesting that carbon flux was successfully directed toward succinyl-CoA and then into the C4 pathway. Also, note that acetogenesis was reduced upon involving glyoxylate shunt (which can bypass decarboxylation associated with the oxidative TCA cycle) for carbon flux direction, improving biosynthesis yields for PBG and porphyrins. Nevertheless, a general trend of the time course of PBG titer remained unchanged, i.e., the PBG titer reached a peak value and then declined toward the end of the cultivation. Such PBG instability, potentially caused by unregulated subsequent reactions toward porphyrins, was alleviated by repression of *hemC* expression via CRISPRi in DMH-D9 Δ *iclR* Δ *sdhA*. PBG (and porphyrin) biosynthesis was further enhanced by heterologous coexpression of *hemA* from *R. spheroides* and the native *E. coli hemB* and, most importantly, all the above metabolic and *hemC*-repression strategies were still functional under this new genetic background, as shown in all corresponding DSL strains. Note that ALA dehydratase (i.e., HemB, encoded by *hemB*) is subject

to feedback inhibition by its downstream metabolite of protoporphyrinogen IX (PPIX) (Zhang et al., 2015), potentially limiting the PBG yield. Repression of *hemC* expression could potentially reduce PPIX formation and its feedback inhibition on *hemB* expression, and subsequently increase PBG formation. The effects of heterologous expression of *hemB* could be clearly observed by much higher peak and final PBG titers between the corresponding DMH and DSL strains. The effects of amplification of various genes in the porphyrin biosynthetic pathway on porphyrin formation were documented (Lee et al., 2013). Note that, under aerobic culture conditions, the PBG yield of DSL-D9 Δ *iclR* Δ *sdhA* with all implemented metabolic and genetic strategies was 2.66-fold that of the control DMH.

Under microaerobic conditions, succinyl-CoA was derived primarily via the reductive TCA branch (Shin et al., 2007) and, therefore, the oxidative TCA cycle had to be inactivated, such as mutating *sdhA* in DMH Δ *sdhA*, to support functional operation of the central metabolism. While PBG can be produced under microaerobic conditions, bioreactor cultivation suffered poor cell growth and glycerol utilization with significant acetogenesis and PBG instability. Interestingly, porphyrin biosynthesis appeared to be more effective under microaerobic conditions (as evidenced by higher absorbance values for Soret peak and Q-band) than aerobic cultivation though PBG biosynthesis showed the opposite. Compared to aerobic cultivation, significant amounts of formate were observed for PBG-producing strains cultivated under microaerobic conditions, presumably due to the induced activity of pyruvate formate lyase (PFL) under oxygen-limited conditions instead of pyruvate dehydrogenase (PDH) which is mostly active in oxygen-rich environment (Durnin et al., 2009). Adverse effects arising from accumulated formate and acetate on culture performance were reported (Kirkpatrick et al., 2001). Nevertheless, the strain engineering strategies developed for aerobic cultivation, specifically heterologous *hemB* expression and

repression of *hemC* expression, were still applicable to microaerobic cultivation though the improving effects were less significant than those under aerobic conditions. Under microaerobic culture conditions, the PBG yield of DSL-D9 Δ *sdhA* with all implemented strain engineering strategies was 1.73-fold that of the control DMH.

This study has several advantages over other reported PBG biosynthesis studies in variety of microbial systems. We utilized glycerol as cheap feedstock for direct PBG biosynthesis, compared to the process of PBG preparation from 5-ALA by pretreated cells of *Chromatium vinosum* (Vogelmann et al., 1975). We attained a PBG concentration of 0.182 mmol/g-DCW in *E. coli* without extraneous supplementation of succinate and glycine. We obtained maximum PBG concentration of 924 μ M compared to 72 μ M from *Propionibacterium freudenreichii* (Y. Z. Piao et al., 2004) or 200 μ M from *Rhodopseudomonas spheroids* (Hatch & Lascelles, 1972).

Chapter 6

Conclusions

In this study, we demonstrated that implementation of the non-native C₄ pathway in *E. coli* was effective to supply carbon flux from the natural TCA pathways for PBG biosynthesis via succinyl-CoA. Metabolic engineering and bioprocessing strategies were further applied for effective carbon flux direction from the TCA pathways to the C₄ pathway for enhanced PBG biosynthesis. To promote PBG accumulation, CRISPRi was successfully applied to repress *hemC* expression with minimal impact to cell physiology. The heterologous expression of the native *E. coli hemB* further enhanced overall PBG biosynthesis which was limited by fusion of two 5-ALA molecules catalyzed by HemB. Overall, we enhanced PBG formation and accumulation in engineered *E. coli* by utilizing a cheap carbon source for direct biosynthesis without precursor supplementation. In addition, potential biochemical, genetic, and metabolic factors limiting PBG production were characterized.

References

- [1]. International Energy Agency, http://www.iea.org/publications/freepublications/publication/KeyWorld_Statistics_2015.pdf [accessed June 2016].
- [2] International Energy Agency. Key world energy, http://www.iea.org/publications/freepublications/publication/KeyWorld2013_FINAL_WEB.pdf. [accessed October 2013]
- Akawi, L., Srirangan, K., Liu, X., Moo-Young, M., & Chou, C. (2015). Engineering *Escherichia coli* for high-level production of propionate. *Journal of Industrial Microbiology & Biotechnology*, 42. <https://doi.org/10.1007/s10295-015-1627-4>
- Anderson, K. E. (2019). Acute hepatic porphyrias: Current diagnosis & management. *Mol Genet Metab*, 128(3), 219-227. <https://doi.org/10.1016/j.ymgme.2019.07.002>
- Baba, T., Ara, T., Hasegawa, M., Takai, Y., Okumura, Y., Baba, M., . . . Mori, H. (2006). Construction of *Escherichia coli* K-12 in-frame, single-gene knockout mutants: the Keio collection. In *Mol Syst Biol*.
- Blankschien, M. D., Clomburg, J. M., & Gonzalez, R. (2010). Metabolic engineering of *Escherichia coli* for the production of succinate from glycerol. *Metab Eng*, 12(5), 409-419. <https://doi.org/10.1016/j.ymben.2010.06.002>
- Cao, Y., Zhang, R., Sun, C., Cheng, T., Liu, Y., & Xian, M. (2013). Fermentative succinate production: an emerging technology to replace the traditional petrochemical processes. *Biomed Res Int*, 2013, 723412. <https://doi.org/10.1155/2013/723412>
- Chen, X., Zhou, L., Tian, K., Kumar, A., Singh, S., Prior, B. A., & Wang, Z. (2013). Metabolic engineering of *Escherichia coli*: a sustainable industrial platform for bio-based chemical production. *Biotechnol Adv*, 31(8), 1200-1223. <https://doi.org/10.1016/j.biotechadv.2013.02.009>
- Cheng, K.-K., Wang, G.-Y., Zeng, J., & Zhang, J.-A. (2013). Improved Succinate Production by Metabolic Engineering. *BioMed Research International*, 2013, 1-12, Article 538790. <https://doi.org/10.1155/2013/538790>

- Cherepanov, P. P., & Wackernagel, W. (1995). Gene disruption in *Escherichia coli*: TcR and KmR cassettes with the option of Flp-catalyzed excision of the antibiotic-resistance determinant. *Gene*, 158(1), 9-14. [https://doi.org/10.1016/0378-1119\(95\)00193-A](https://doi.org/10.1016/0378-1119(95)00193-A)
- Ciriminna, R., Pina, C. D., Rossi, M., & Pagliaro, M. (2014). Understanding the glycerol market. *European Journal of Lipid Science and Technology*, 116(10), 1432-1439. <https://doi.org/10.1002/ejlt.201400229>
- Dailey, H. A., Dailey, T. A., Gerdes, S., Jahn, D., Jahn, M., O'Brian, M. R., & Warren, M. J. (2017). Prokaryotic Heme Biosynthesis: Multiple Pathways to a Common Essential Product. *Microbiol Mol Biol Rev*, 81(1). <https://doi.org/10.1128/MMBR.00048-16>
- Datsenko, K. A., & Wanner, B. L. (2000). One-step inactivation of chromosomal genes in *Escherichia coli* K-12 using PCR products. *Proceedings of the National Academy of Sciences*, 97(12), 6640-6645.
- de Verneuil, H., Sassa, S., & Kappas, A. (1983). Purification and properties of uroporphyrinogen decarboxylase from human erythrocytes. A single enzyme catalyzing the four sequential decarboxylations of uroporphyrinogens I and III. *J Biol Chem*, 258(4), 2454-2460. <https://www.ncbi.nlm.nih.gov/pubmed/6822570>
- Demirbas, A. (2011). Competitive liquid biofuels from biomass. *Applied Energy*, 88(1), 17-28. <https://doi.org/10.1016/j.apenergy.2010.07.016>
- Dharmadi, Y., Murarka, A., & Gonzalez, R. (2006). Anaerobic fermentation of glycerol by *Escherichia coli*: a new platform for metabolic engineering. *Biotechnol Bioeng*, 94(5), 821-829. <https://doi.org/10.1002/bit.21025>
- Durnin, G., Clomburg, J., Yeates, Z., Alvarez, P. J., Zygorakis, K., Campbell, P., & Gonzalez, R. (2009). Understanding and harnessing the microaerobic metabolism of glycerol in *Escherichia coli*. *Biotechnol Bioeng*, 103(1), 148-161. <https://doi.org/10.1002/bit.22246>
- Farrell, C. C., Osman, A. I., Doherty, R., Saad, M., Zhang, X., Murphy, A., . . . Rooney, D. W. (2020). Technical challenges and opportunities in realising a circular economy for waste photovoltaic modules. *Renewable & Sustainable Energy Reviews*, 128. <https://doi.org/ARTN 109911>

10.1016/j.rser.2020.109911

- Frankenberg, N., Moser, J., & Jahn, D. (2003). Bacterial heme biosynthesis and its biotechnological application. *Appl Microbiol Biotechnol*, 63(2), 115-127. <https://doi.org/10.1007/s00253-003-1432-2>
- Frydman, B., Despuy, M. E., & Rapoport, H. (1965). Pyrroles from Azaindoles. A Synthesis of Porphobilinogen. *J Am Chem Soc*, 87, 3530-3531. <https://doi.org/10.1021/ja01093a061>
- Frydman, B., Reil, S., Despuy, M. E., & Rapoport, H. (1969). Pyrroles from azaindoles. A synthesis of porphobilinogen and related pyrroles. *J Am Chem Soc*, 91(9), 2338-2342. <https://doi.org/10.1021/ja01037a025>
- Gibson, S. L., Mackenzie, J. C., & Goldberg, A. (1968). The diagnosis of industrial lead poisoning. *Br J Ind Med*, 25(1), 40-51. <https://doi.org/10.1136/oem.25.1.40>
- Gonzalez, R., Murarka, A., Dharmadi, Y., & Yazdani, S. S. (2008). A new model for the anaerobic fermentation of glycerol in enteric bacteria: trunk and auxiliary pathways in *Escherichia coli*. *Metab Eng*, 10(5), 234-245. <https://doi.org/10.1016/j.ymben.2008.05.001>
- Guo, F., Jia, X., Liang, S., Zhou, N., Chen, P., & Ruan, R. (2020). Development of biochar-based nanocatalysts for tar cracking/reforming during biomass pyrolysis and gasification. *Bioresour Technol*, 298, 122263. <https://doi.org/10.1016/j.biortech.2019.122263>
- Hatch, T., & Lascelles, J. (1972). Accumulation of porphobilinogen and other pyrroles by mutant and wild type *Rhodospseudomonas spheroides*: regulation by heme. *Archives of Biochemistry and Biophysics*, 150(1), 147-153. [https://doi.org/10.1016/0003-9861\(72\)90021-5](https://doi.org/10.1016/0003-9861(72)90021-5)
- Hermann, T. (2003). Industrial production of amino acids by coryneform bacteria. *J Biotechnol*, 104(1-3), 155-172. [https://doi.org/10.1016/s0168-1656\(03\)00149-4](https://doi.org/10.1016/s0168-1656(03)00149-4)
- Hevekerl, A., Kuenz, A., & Vorlop, K. D. (2014). Influence of the pH on the itaconic acid production with *Aspergillus terreus*. *Appl Microbiol Biotechnol*, 98(24), 10005-10012. <https://doi.org/10.1007/s00253-014-6047-2>
- Jackson, A., & MacDonald, S. (1957). Synthesis of porphobilinogen. *Canadian Journal of Chemistry*, 35(7), 715-722.
- Jacobi, P. A., & Li, Y. K. (2001). Synthesis of porphobilinogen via a novel ozonide cleavage reaction. *Journal of the American Chemical Society*, 123(38), 9307-9312. <https://doi.org/10.1021/ja016303q>

- Jahn, D., Verkamp, E., & Soll, D. (1992). Glutamyl-transfer RNA: a precursor of heme and chlorophyll biosynthesis. *Trends Biochem Sci*, 17(6), 215-218. [https://doi.org/10.1016/0968-0004\(92\)90380-r](https://doi.org/10.1016/0968-0004(92)90380-r)
- Jobling, M. G., & Holmes, R. K. (1990). Construction of vectors with the p15a replicon, kanamycin resistance, inducible lacZ alpha and pUC18 or pUC19 multiple cloning sites. *Nucleic acids research*, 18(17), 5315-5316. <https://doi.org/10.1093/nar/18.17.5315>
- Jones, M. I., Froussios, C., & Evans, D. A. (1976). A short, versatile synthesis of porphobilinogen [10.1039/C39760000472]. *Journal of the Chemical Society, Chemical Communications*(12), 472-473. <https://doi.org/10.1039/C39760000472>
- Kargbo, H., Harris, J. S., & Phan, A. N. (2021). "Drop-in" fuel production from biomass: Critical review on techno-economic feasibility and sustainability. *Renewable & Sustainable Energy Reviews*, 135. <https://doi.org/ARTN 110168>
- 10.1016/j.rser.2020.110168
- Kenner, G. W., Rimmer, J., Smith, K. M., & Unsworth, J. F. (1977). Pyrroles and related compounds. Part 38. Porphobilinogen synthesis. *J Chem Soc Perkin 1*(3), 332-340. <https://www.ncbi.nlm.nih.gov/pubmed/557056>
- Kirkpatrick, C., Maurer, L. M., Oyelakin, N. E., Yoncheva, Y. N., Maurer, R., & Slonczewski, J. L. (2001). Acetate and formate stress: opposite responses in the proteome of Escherichia coli. *J Bacteriol*, 183(21), 6466-6477. <https://doi.org/10.1128/JB.183.21.6466-6477.2001>
- Kwon, S. J., de Boer, A. L., Petri, R., & Schmidt-Dannert, C. (2003). High-level production of porphyrins in metabolically engineered Escherichia coli: systematic extension of a pathway assembled from overexpressed genes involved in heme biosynthesis. *Appl Environ Microbiol*, 69(8), 4875-4883. <https://doi.org/10.1128/AEM.69.8.4875-4883.2003>
- Labun, K., Montague, T. G., Gagnon, J. A., Thyme, S. B., & Valen, E. (2016). CHOPCHOP v2: a web tool for the next generation of CRISPR genome engineering. *Nucleic acids research*, 44(W1), W272-W276.
- Layer, G., Reichelt, J., Jahn, D., & Heinz, D. W. (2010). Structure and function of enzymes in heme biosynthesis. *Protein Sci*, 19(6), 1137-1161. <https://doi.org/10.1002/pro.405>
- Lee, M. J., Kim, H. J., Lee, J. Y., Kwon, A. S., Jun, S. Y., Kang, S. H., & Kim, P. (2013). Effect of gene amplifications in porphyrin pathway on heme biosynthesis in a recombinant

- Escherichia coli. *J Microbiol Biotechnol*, 23(5), 668-673.
<https://doi.org/10.4014/jmb.1302.02022>
- Lu, J., Sheahan, C., & Fu, P. C. (2011). Metabolic engineering of algae for fourth generation biofuels production. *Energy & Environmental Science*, 4(7), 2451-2466.
<https://doi.org/10.1039/c0ee00593b>
- Mathews, M. A., Schubert, H. L., Whitby, F. G., Alexander, K. J., Schadick, K., Bergonia, H. A., . . . Hill, C. P. (2001). Crystal structure of human uroporphyrinogen III synthase. *EMBO J*, 20(21), 5832-5839. <https://doi.org/10.1093/emboj/20.21.5832>
- Mauzerall, D., & Granick, S. (1956). THE OCCURRENCE AND DETERMINATION OF δ -AMINOLEVULINIC ACID AND PORPHOBILINOGEN IN URINE. *Journal of Biological Chemistry*, 219(1), 435-446. <http://www.jbc.org/content/219/1/435.short>
- Miller, J. H. (1992). *A short course in bacterial genetics: a laboratory manual and handbook for Escherichia coli and related bacteria*. Cold Spring Harbor Laboratory Press.
- Miscevic, D., Mao, J. Y., Kefale, T., Abedi, D., Moo-Young, M., & Perry Chou, C. (2021). Strain engineering for high-level 5-aminolevulinic acid production in Escherichia coli. *Biotechnol Bioeng*, 118(1), 30-42. <https://doi.org/10.1002/bit.27547>
- Miscevic, D., Mao, J. Y., Moo-Young, M., & Chou, C. P. (2020). High-level heterologous production of propionate in engineered Escherichia coli. *Biotechnol Bioeng*, 117(5), 1304-1315. <https://doi.org/10.1002/bit.27276>
- Naik, S. N., Goud, V. V., Rout, P. K., & Dalai, A. K. (2010). Production of first and second generation biofuels: A comprehensive review. *Renewable & Sustainable Energy Reviews*, 14(2), 578-597. <https://doi.org/10.1016/j.rser.2009.10.003>
- Nandi, D. L. (1978). Delta-aminolevulinic acid synthase of rhodospseudomonas spheroides. Binding of pyridoxal phosphate to the enzyme. *Arch Biochem Biophys*, 188(2), 266-271.
[https://doi.org/10.1016/s0003-9861\(78\)80008-3](https://doi.org/10.1016/s0003-9861(78)80008-3)
- Neidhardt, F. C., Bloch, P. L., & Smith, D. F. (1974). Culture Medium for Enterobacteria. *Journal of Bacteriology*, 119(3), 736-747. <http://jb.asm.org/content/119/3/736.abstract>
- Neier, R. (2000). A novel synthesis of porphobilinogen: Synthetic and biosynthetic studies. *Journal of Heterocyclic Chemistry*, 37, 487-508.

- Osman, A. I., Hefny, M., Maksoud, M. I. A. A., Elgarahy, A. M., & Rooney, D. W. (2021). Recent advances in carbon capture storage and utilisation technologies: a review. *Environmental Chemistry Letters*, 19(2), 797-849. <https://doi.org/10.1007/s10311-020-01133-3>
- Papagianni, M. (2007). Advances in citric acid fermentation by *Aspergillus niger*: biochemical aspects, membrane transport and modeling. *Biotechnol Adv*, 25(3), 244-263. <https://doi.org/10.1016/j.biotechadv.2007.01.002>
- Pengpumkiat, S., Koesdjojo, M., Rowley, E. R., Mockler, T. C., & Remcho, V. T. (2016). Rapid Synthesis of a Long Double-Stranded Oligonucleotide from a Single-Stranded Nucleotide Using Magnetic Beads and an Oligo Library. *PLoS one*, 11(3), e0149774-e0149774. <https://doi.org/10.1371/journal.pone.0149774>
- Piao, Y., Kiatpapan, P., Yamashita, M., & Murooka, Y. (2004). Effects of expression of hemA and hemB genes on production of porphyrin in *Propionibacterium freudenreichii*. *Appl Environ Microbiol*, 70(12), 7561-7566. <https://doi.org/10.1128/AEM.70.12.7561-7566.2004>
- Piao, Y. Z., Kiatpapan, P., Yamashita, M., & Murooka, Y. (2004). Effects of expression of hemA and hemB Genes on production of porphyrin in *Propionibacterium freudenreichii*. *Applied and Environmental Microbiology*, 70(12), 7561-7566. <https://doi.org/10.1128/Aem.70.12.7561-7566.2004>
- Qi, L. S., Larson, M. H., Gilbert, L. A., Doudna, J. A., Weissman, J. S., Arkin, A. P., & Lim, W. A. (2013). Repurposing CRISPR as an RNA-guided platform for sequence-specific control of gene expression. *Cell*, 152(5), 1173-1183. <https://doi.org/10.1016/j.cell.2013.02.022>
- Reid, W. V., Ali, M. K., & Field, C. B. (2020). The future of bioenergy. *Glob Chang Biol*, 26(1), 274-286. <https://doi.org/10.1111/gcb.14883>
- Shin, Jeong-Ah, Kwon, Y. D., Kwon, O. R., Lee, E. S., & Kim, P. (2007). 5-aminolevulinic acid biosynthesis in *Escherichia coli* coexpressing NADP-dependent malic enzyme and 5-aminolevulinic synthase. *Journal of Microbiology and Biotechnology*, 17(9), 1579-1584. <Go to ISI>://WOS:000249875200025
- Sikarwar, V. S., Zhao, M., Fennell, P. S., Shah, N., & Anthony, E. J. (2017). Progress in biofuel production from gasification. *Progress in Energy and Combustion Science*, 61, 189-248. <https://doi.org/10.1016/j.pecs.2017.04.001>

- Singh, A., Olsen, S. I., & Nigam, P. S. (2011). A viable technology to generate third-generation biofuel. *Journal of Chemical Technology and Biotechnology*, 86(11), 1349-1353. <https://doi.org/10.1002/jctb.2666>
- Srirangan, K., Liu, X., Westbrook, A., Akawi, L., Pyne, M. E., Moo-Young, M., & Chou, C. P. (2014). Biochemical, genetic, and metabolic engineering strategies to enhance coproduction of 1-propanol and ethanol in engineered *Escherichia coli*. *Appl Microbiol Biotechnol*, 98(22), 9499-9515. <https://doi.org/10.1007/s00253-014-6093-9>
- Srirangan, K., Liu, X., Westbrook, A., Akawi, L., Pyne, M. E., Moo-Young, M., & Chou, C. P. (2014). Biochemical, genetic, and metabolic engineering strategies to enhance coproduction of 1-propanol and ethanol in engineered *Escherichia coli*. *Applied Microbiology and Biotechnology*, 98(22), 9499-9515.
- Thakker, C., Martinez, I., San, K. Y., & Bennett, G. N. (2012). Succinate production in *Escherichia coli*. *Biotechnol J*, 7(2), 213-224. <https://doi.org/10.1002/biot.201100061>
- Ullah, K., Ahmad, M., Sofia, Sharma, V. K., Lu, P. M., Harvey, A., . . . Sultana, S. (2015). Assessing the potential of algal biomass opportunities for bioenergy industry: A review. *Fuel*, 143, 414-423. <https://doi.org/10.1016/j.fuel.2014.10.064>
- Vogelmann, H., Ghahremani, B., & Wagner, F. (1975). Preparation of porphobilinogen and uroporphyrin III from δ -aminolaevulinic acid by pretreated cells of *Chromatium vinosum*. *European journal of applied microbiology and biotechnology*, 2(1), 19-28.
- Vuoristo, K. S., Mars, A. E., Sanders, J. P. M., Eggink, G., & Weusthuis, R. A. (2016). Metabolic Engineering of TCA Cycle for Production of Chemicals. *Trends Biotechnol*, 34(3), 191-197. <https://doi.org/10.1016/j.tibtech.2015.11.002>
- Westall, R. G. (1952). Isolation of porphobilinogen from the urine of a patient with acute porphyria. *Nature*, 170(4328), 614-616. <https://doi.org/10.1038/170614a0>
- Westbrook, A. W., Miscevic, D., Kilpatrick, S., Bruder, M. R., Moo-Young, M., & Chou, C. P. (2019). Strain engineering for microbial production of value-added chemicals and fuels from glycerol. *Biotechnol Adv*, 37(4), 538-568. <https://doi.org/10.1016/j.biotechadv.2018.10.006>
- Yim, H., Haselbeck, R., Niu, W., Pujol-Baxley, C., Burgard, A., Boldt, J., . . . Van Dien, S. (2011). Metabolic engineering of *Escherichia coli* for direct production of 1,4-butanediol. *Nat Chem Biol*, 7(7), 445-452. <https://doi.org/10.1038/nchembio.580>

Zhang, J., Kang, Z., Chen, J., & Du, G. (2015). Optimization of the heme biosynthesis pathway for the production of 5-aminolevulinic acid in *Escherichia coli*. *Sci Rep*, 5, 8584. <https://doi.org/10.1038/srep08584>

Appendix A: Supplementary Tables

Table S1: DNA oligonucleotide sequences used in this study





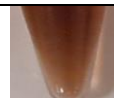
















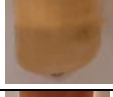











































































Primers/oligo name	Primer/oligo sequence (Top DNA strand 5' → 3')	Source
v-ldhA	GATAACGGAGATCGGGAATGATTAA; GGTTTAAAAGCGTCGATGTCCAGTA	(Akawi et al., 2015)
v-sdhA	CTCTGCGTTCACCAAAGTGT; ACACACCTTCACGGCAGGAG	(Miscevic et al., 2021)
v-iclR	GGTGGAATGAGATCTTGCGA; CCGACACGCTCAACCCAGAT	(Miscevic et al., 2021)
c-frm	AGATTGCAGCATTACACGTCCTTGAG; CCAGCTGCATTAATGAATCGGGCCATGGTCCATATGAATATCCTCC	(Kajan Srirangan et al., 2014)
c-ptrc	CCGATTCATTAATGCAGCTGG; GGTCTGTTTCCTGTGTGAAATTGTTA	(Kajan Srirangan et al., 2014)
cf-gRNA	ATCTTTGACAGCTAGCTCAGTCC; CAAGCTTCAAAAAAAGCACCGA	(Miscevic et al., 2021)
q-hemC	TCCAGTTTACGTCCAGTG; AATACCCACCGCACCTTGTC	This study
q-rrsA	AACTGGAGGAAGGTGGGGAT; TCACCGTGGCATTCTGATCC	This study
g-hemA	CACAGAAACAGCTATGACCATGGACTACAATCTGGCACTCGA; GAGCTCGAATTCGTAATCATTACAGGCAACGACCTCGGC	(Miscevic et al., 2021)
g-pK-hemA	GCGCCGAGGTCGTTGCCTGAATGATTACGAATTCGAGCTCGGTAC; AGTGCCAGATTGTAGTCCATGGTCATAGCTGTTTCCTGTGTG	(Miscevic et al., 2021)
g-hemA-hemB	CCGAGGTCGTTGCCTGAATTTACACAGGAAACAGACCATGACAGACTTAATCC; ACCGAGCTCGAATTCGTAATCATTTAACGCAGAATCTTCTTCAGCC	This study
g-pK-hemA-hemB	TTAAGTCTGTCATGGTCTGTTTCCTGTGTGAAATTCAGGCAACGACCTCGG; CTGAGAAGAAGATTCTGCGTTAAATGATTACGAATTCGAGCTCGGTACC	This study
cf-pK-hemA	AACAGCTATGACCATGGACTAC; ATTCGTAATCATTACAGGCAACG	This study
cf-pK-hemA-hemB	AACAGCTATGACCATGGACTAC; TTCGTAATCATTTAACGCAGAAT	This study
g-pgRNA	GTTTTAGAGCTAGAAATAGCAAGTT; ACTAGTATTATACCTAGGACTGAGC	(Miscevic et al., 2021)
hemC-gRNA-D1	GTCCTAGGTATAAATACTAGTCTCTGGCAAGGATGTTAGGAGTTTTAGAGCTAGAAATAGC; GCTATTTCTAGCTCTAAAAC <u>TCCTAACATCCTTGCCAGAG</u> ACTAGTATTATACCTAGGAC	This study
hemC-gRNA-D2	GTCCTAGGTATAAATACTAGT <u>GTTACCGTCATTATCATCCG</u> GTTTTAGAGCTAGAAATAGC; GCTATTTCTAGCTCTAAAACCGGATGATAATGACGGTAACACTAGTATTATACCTAGGAC	This study
hemC-gRNA-D3	GTCCTAGGTATAAATACTAGT <u>AGACCTTGCGGGAATTCAACG</u> TTTTAGAGCTAGAAATAGC; GCTATTTCTAGCTCTAAAACGTTGAATTCGCAAGGCTACTAGTATTATACCTAGGAC	This study
hemC-gRNA-D4	GTCCTAGGTATAAATACTAGT <u>AGCTTATTGATGGCGAAATCG</u> TTTTAGAGCTAGAAATAGC; GCTATTTCTAGCTCTAAAACGATTTCCGCAATCAATAAGCTACTAGTATTATACCTAGGAC	This study
hemC-gRNA-D5	GTCCTAGGTATAAATACTAGT <u>ACACTGACATCACTCTGGCAG</u> TTTTAGAGCTAGAAATAGC; GCTATTTCTAGCTCTAAAAC <u>TGCCAGAGTGATGTCAGTGT</u> ACTAGTATTATACCTAGGAC	This study
hemC-gRNA-D6	GTCCTAGGTATAAATACTAGT <u>CGACGTTGCCGCGCAGGGAG</u> GTTTTAGAGCTAGAAATAGC; GCTATTTCTAGCTCTAAAACCTCCCTGCGCGCAACGTCGACTAGTATTATACCTAGGAC	This study
hemC-gRNA-D7	GTCCTAGGTATAAATACTAGT <u>AGAAATCTCGGGTGGCAACG</u> GTTTTAGAGCTAGAAATAGC; GCTATTTCTAGCTCTAAAACCGTTGCCACCCGAGATTTCTACTAGTATTATACCTAGGAC	This study
hemC-gRNA-D8	GTCCTAGGTATAAATACTAGT <u>CGCCTGAGCAA</u> ACTGGATAAGTTTTAGAGCTAGAAATAGC; GCTATTTCTAGCTCTAAAAC <u>TTATCCAGTTTGCTCAGGCG</u> ACTAGTATTATACCTAGGAC	This study
hemC-gRNA-D9	GTCCTAGGTATAAATACTAGT <u>TTGGCACTGGCGACG</u> TAAACGTTTTAGAGCTAGAAATAGC; GCTATTTCTAGCTCTAAAAC <u>GTTTACGTCCAGTGCCAA</u> ACTAGTATTATACCTAGGAC	This study

Notation for oligonucleotides: v-verification primer, c-cloning primer, cf- confirmation primer, q-reverse transcription primers, and g-Gibson DNA assembly primer. 20 nt *hemC*-targeting sequence is underlined.

Table S2: gRNA sequences targeting *hemC* for CRISPRi in this study. See Figure S1 for qRT-PCR results for select gRNAs.

gRNA	20 nt targeting sequence	sgRNA location on <i>hemC</i> gene	Predicted % expression efficiency	% GC Content	RQ for <i>hemC</i> expression (From qRT-PCR)
<i>hemC</i> -gRNA-D1	CTCTGGCAAGGATGTTAGGA	-150	43.6	50	-
<i>hemC</i> -gRNA-D2	GTTACCGTCATTATCATCCG	-174	57.9	45	-
<i>hemC</i> -gRNA-D3	AGACCTTGCGGGAATTCAAC	+456	48.4	50	-
<i>hemC</i> -gRNA-D4	AGCTTATTGATGGCGAAATC	+952	39.2	40	-
<i>hemC</i> -gRNA-D5	ACACTGACATCACTCTGGCA	-138	65.4	50	1.27
<i>hemC</i> -gRNA-D6	CGACGTTGCCGCGCAGGGAG	+635	49.6	75	0.06
<i>hemC</i> -gRNA-D7	AGAAATCTCGGGTGGCAACG	+754	65.5	55	-
<i>hemC</i> -gRNA-D8	CGCCTGAGCAAACCTGGATAA	+663	57.9	50	-
<i>hemC</i> -gRNA-D9	TTGGCACTGGCGACGTAAAC	+583	26.9	55	0.128

Table S3: Tabulated images of bioreactor cultivation samples under aerobic and microaerobic conditions

Strain Name	0 hr	13-14 hr	18-19 hr	23-24 hr	37-39 hr	42-44 hr	47-48 hr	61-63 hr	Final PBG titer (mg L ⁻¹) ^a	
DMH						N/A			75.1 ± 1.5 (0.65%)	Aerobic
DMHΔ<i>sdhA</i>									115 ± 2.0 (1.01%)	
DMHΔ<i>iclR</i>									80.7 ± 0.4 (0.69%)	
DMHΔ<i>iclR</i>Δ<i>sdhA</i>									87.3 ± 0.3 (0.66%)	
DMH-D9Δ<i>iclR</i>Δ<i>sdhA</i>									140.2 ± 1.8 (1.22%)	
DSL									65.7 ± 3.7 (0.52%)	
DSLΔ<i>sdhA</i>									66.3 ± 2.2 (0.58%)	
DSLΔ<i>iclR</i>									86.6 ± 0.1 (0.72%)	
DSLΔ<i>iclR</i>Δ<i>sdhA</i>									104 ± 1.4 (0.81%)	
DSL-D9Δ<i>iclR</i>Δ<i>sdhA</i>									209 ± 0.3 (1.73%)	
DMH									48.7 ± 0.6 (0.41%)	Micro-aerobic
DMHΔ<i>sdhA</i>									55.9 ± 0.6 (0.46%)	
DMH-D9Δ<i>sdhA</i>									62.5 ± 2.1 (0.53%)	
DSL									57.9 ± 1.2 (0.54%)	
DSLΔ<i>sdhA</i>							N/A		67.2 ± 0.9 (0.61%)	
DSL-D9Δ<i>sdhA</i>									83.8 ± 0.2 (0.71)	

^a PBG extracellular accumulation (mg L⁻¹) after complete consumption of glycerol, theoretical percent yield based on consumed glycerol is presented in parentheses

N/A not applicable

Table S4: Statistical analysis for comparing experimental data of PBG titers

Group #1		Group #2		P-value	Statistical significance
Strain name	PBG (mg L ⁻¹)	Strain name	PBG (mg L ⁻¹)		
Aerobic Conditions					
DMH	75.1 ± 1.5	DMHΔ <i>sdhA</i>	115 ± 2.0	0.0015	<i>P</i> < 0.05*
DMH	75.1 ± 1.5	DMHΔ <i>iclR</i>	80.7 ± 0.4	0.104	<i>P</i> > 0.05
DMH	75.1 ± 1.5	DMHΔ <i>iclR</i> Δ <i>sdhA</i>	87.3 ± 0.3	0.049	<i>P</i> < 0.05*
DMH	75.1 ± 1.5	DMH-D9Δ <i>iclR</i> Δ <i>sdhA</i>	140.2 ± 1.8	0.0008	<i>P</i> < 0.05*
DMHΔ <i>iclR</i> Δ <i>sdhA</i>	87.3 ± 0.3	DMH-D9Δ <i>iclR</i> Δ <i>sdhA</i>	140.2 ± 1.8	0.0132	<i>P</i> < 0.05*
DSL	65.7 ± 3.7	DSLΔ <i>sdhA</i>	66.3 ± 2.2	0.860	<i>P</i> > 0.05
DSL	65.7 ± 3.7	DSLΔ <i>iclR</i>	86.6 ± 0.1	0.041	<i>P</i> < 0.05*
DSL	65.7 ± 3.7	DSLΔ <i>iclR</i> Δ <i>sdhA</i>	104 ± 1.4	0.024	<i>P</i> < 0.05*
DSL	65.7 ± 3.7	DSL-D9Δ <i>iclR</i> Δ <i>sdhA</i>	209 ± 0.3	0.011	<i>P</i> < 0.05*
DSLΔ <i>iclR</i> Δ <i>sdhA</i>	104 ± 1.4	DSL-D9Δ <i>iclR</i> Δ <i>sdhA</i>	209 ± 0.3	0.004	<i>P</i> < 0.05*
DMH	75.1 ± 1.5	DSL	65.7 ± 3.7	0.133	<i>P</i> > 0.05
DMHΔ <i>iclR</i> Δ <i>sdhA</i>	87.3 ± 0.3	DSLΔ <i>iclR</i> Δ <i>sdhA</i>	104 ± 1.4	0.030	<i>P</i> < 0.05*
DMH	75.1 ± 1.5	DSL-D9Δ <i>iclR</i> Δ <i>sdhA</i>	209 ± 0.3	0.003	<i>P</i> < 0.05*
Microaerobic Conditions					
DMH	48.7 ± 0.6	DMHΔ <i>sdhA</i>	55.9 ± 0.6	0.007	<i>P</i> < 0.05*
DMH	48.7 ± 0.6	DMH-D9Δ <i>sdhA</i>	62.5 ± 2.1	0.053	<i>P</i> > 0.05
DMHΔ <i>sdhA</i>	55.9 ± 0.6	DMH-D9Δ <i>sdhA</i>	62.5 ± 2.1	0.122	<i>P</i> > 0.05
DSL	57.9 ± 1.2	DSLΔ <i>sdhA</i>	67.2 ± 0.9	0.017	<i>P</i> < 0.05*
DSL	57.9 ± 1.2	DSL-D9Δ <i>sdhA</i>	83.8 ± 0.2	0.018	<i>P</i> < 0.05*
DSLΔ <i>sdhA</i>	67.2 ± 0.9	DSL-D9Δ <i>sdhA</i>	83.8 ± 0.2	0.018	<i>P</i> < 0.05*
DMH	48.7 ± 0.6	DSL	57.9 ± 1.2	0.027	<i>P</i> < 0.05*
DMHΔ <i>sdhA</i>	55.9 ± 0.6	DSLΔ <i>sdhA</i>	67.2 ± 0.9	0.006	<i>P</i> < 0.05*
DMH	48.7 ± 0.6	DSL-D9Δ <i>sdhA</i>	83.8 ± 0.2	0.004	<i>P</i> < 0.05*

* Difference between two means is considered to be statistically significant